Thiolated arsenic species observed in rice paddy pore waters

Thiolated arsenic species observed in rice paddy pore waters

Jiajia Wang[1], Carolin F. Kerl[1], Pengjie Hu[2], Maria Martin[3], Tingting Mu[2], Lena Brüggenwirth[1], Guangmei Wu[2], Daniel Said-Pullicino[3], Marco Romani[4], Longhua Wu[2] and Britta Planer-Friedrich[1]*

[1]Environmental Geochemistry, Bayreuth Center for Ecology and Environmental Research (BayCEER), University of Bayreuth, 95440 Bayreuth, Germany.

[2]Key Laboratory of Soil Environment and Pollution Remediation, Institute of Soil Science, Chinese Academy of Sciences, 210008 Nanjing, China

[3]Department of Agriculture, Forest and Food Sciences, University of Turin, 10124 Turin, Italy

[4]Rice Research Centre, Ente Nazionale Risi, 27030 Castello d'Agogna, Pavia, Italy

*Phone: +49 921 55 3999. E-mail: b.planer-friedrich@uni-bayreuth.de.

Rice is the main staple crop in the world, yet, the accumulation of carcinogenic arsenic (As) in rice grains represents a health threat to millions of people. Current research only focuses on inorganic and methylated oxyarsenic species. Based on results from field, mesocosm, and soil incubation studies across multiple paddy soils from the major rice cultivation areas in Italy, France, and China, we hereby introduce thioarsenates as further important As species in paddy soil pore-waters. Thioarsenates were observed throughout the cropping season, with concentrations comparable to the much-better-investigated methylated oxyarsenates. Anaerobic soil incubations confirmed a large potential for thiolation across a wide diversity of paddy soil types originating from different climate zones and parent materials. Occurrence of inorganic thioarsenates was predominantly related to soil pH > 6.5 and controlled by the presence of zero-valent sulfur, while occurrence of methylated thioarsenates was predominantly observed at soil pH < 7 and related to the presence of their precursors, methylated oxyarsenates. High concentrations of dissolved iron limited As thiolation. Sulfate fertilization increased thioarsenate formation. Our results highlight thiolation as an important factor to As biogeochemistry in rice paddies but it is yet unknown whether thiolation is boon or bane for rice safety.

Rice is the main staple crop for more than half of the World´s population. At the same time, it represents a major dietary source of arsenic (As), a class I carcinogen [1]. Premises for As accumulation in rice grains are its global occurrence in soils and efficient uptake by rice plants together with essential nutrients [2, 3, 4]. Soil-derived As becomes plant-available under flooded conditions when the reductive dissolution of iron (Fe) (oxy)hydroxides and arsenate reduction release sorbed As [5]. Pore-water As speciation is dominated by inorganic As (arsenite and arsenate). Microbe-mediated As methylation leads to formation of mono- (MMA) and dimethylarsenate (DMA) [6] which typically are minor species in pore-waters [7], although DMA can contribute up to 90% of total As in the grain due to high root-shoot translocation [8]. Current research on As biogeochemistry in paddy soils mainly has been focusing on these four oxyarsenic species and it is well-accepted that As speciation is responsible for its mobility and bioavailability [9].

Our objective was to reveal whether and to what extent thioarsenates contribute to As speciation in paddy soil pore-waters. Thioarsenates are pentavalent As species in which sulfur (S) replaces oxygen. They form upon reaction of arsenite with zero-valent S and sulfide (in case of inorganic thioarsenates) [10], or MMA and DMA with sulfide (in case of methylated thioarsenates) [11, 12] (Fig. 1). Thioarsenates typically occur in aquatic environments with excess dissolved sulfide [13]. Just very recently they have also been detected in low sulfide environments where thiolation is probably controlled by reactions with reduced S bound to surfaces of minerals or organic matter [10, 14].

To date, occurrence of thioarsenates in paddy soils has never been addressed which is only partially a methodological problem. Routine sample preservation and many chromatographic separation methods use acids which transform thioarsenates to

arsenite or oxyarsenates [15] or lead to As loss by As-S precipitation [16], so thioarsenates are plainly overlooked. However, the main reason for neglectance of thioarsenates is a conceptual limitation because flooded paddy soils are primarily regarded as methanogenic environments [17]. Sulfate reduction, though thermodynamically favored relative to methanogenesis, is often considered insignificant due to typically low (except for acid sulfate soils) sulfate contents [18], and sulfide reactivity being limited by mackinawite ($Fe^{II}S$) precipitation [19]. There is, however, evidence for a "cryptic" S-cycle [18], where sulfide re-oxidation to zero-valent S is coupled to reduction of Fe(III) (oxy)hydroxides and formation of mixed $Fe^{II}Fe^{III}$ minerals or pyrite ($Fe^{II}S_2$) besides Fe^{2+} [20]. Further S oxidation to thiosulfate and sulfate is coupled to nitrate or oxygen reduction (Fig. 1). Such a S-cycle sustains high sulfate reduction rates in the bulk soil and especially the rhizosphere [18]. We hypothesized that low but continuously replenished sulfide and zero-valent S could promote thioarsenate formation besides or instead of As scavenging on newly formed Fe minerals [21]. A similar observation was made in paddy soil incubation studies where initially sequestered As was remobilized under sulfidic conditions [22]. Thioarsenate formation was suspected, but no As-S speciation analysis was done. Sulfate fertilization, recently investigated for its potential benefits in improving nutrient uptake and rice growth [23], as well as mitigating methane emissions [24, 25] and rice As accumulation [26, 27], might further contribute to thioarsenate formation.

During an initial field survey, we had discovered thioarsenates while sampling planted paddy fields covering the main rice cropping areas of the river Po plain in Italy (soil pH 5.0-6.1, As 5.1-16 mg/kg), and of the Camargue coastal plain in France (soil pH 7.5-7.6, As 10.4-20.2 mg/kg). Contribution of total thiolation to total As concentrations was 8.3% at maximum and 2.1% on average; numbers comparable to

those observed for the much more-commonly-investigated methylated oxyarsenates (for details see supporting information section 1, Table S1, Fig. S1-S4).

Key to all further investigations was the development of a novel sampling and analytical method using diethylenetriamine-pentaacetic acid (DTPA, 10 mM) to complex excess dissolved Fe, followed by flash-freezing for sample preservation, sample dilution and the use of an adapted eluent for chromatographic separation to avoid negative effects of high DTPA concentrations such as retention time shifts, peak splitting, and poor species resolution. Detection limits of the optimized method were 0.03 µg/L As and recovery rates >80%, which is the currently by far best available stabilization and analysis method for detection of the up to 11 species of interest (see methods´ section for details).

We then examined occurrence of inorganic and methylated thioarsenates in comparison to their oxyarsenic analogues over a range of scales moving from our initial field surveys to controlled mesocosm experiments and laboratory soil incubations.

Thioarsenate formation in rice cultivation mesocosms.

Based on the field survey (Table S1), we selected two Italian paddy soils (an Eutric Gleysol from a paddy field near Cascina Veronica and an Umbric Gleysol from a paddy field near Cascina Fornazzo), characterized by highest proportions of thiolation, for mesocosm experiments (setup see Fig. S5). The two soils had the same total soil As contents (5.5 mg/kg) and were relatively similar in soil pH (5.6 and 5.8 for Veronica and Fornazzo, respectively), while in comparison to Fornazzo, Veronica had slightly lower contents of 0.5 M HCl-extractable Fe (52 vs. 71

mmol/kg), total C (2.0 vs. 4.7 %), and total S (2.6 vs. 3.2 g/kg) (Table S2). All mesocosms were planted with the same rice variety (*Oryza sativa* L. cv. Selenio) and managed in a completely randomized factorial arrangement representing (i) treated with (S) or without sulfate (no S, control) fertilizers and (ii) water or dry seeded (Fig. S5, S6). In water seeded treatments soils were flooded from one day before seeding throughout the growing season, while in dry seeded treatments oxic soil conditions were maintained until tillering stage (20 days after seeding) after which the soils were flooded (Fig. S6). Consequently, dry seeded soils showed higher redox potentials and lower pore-water Fe(II) concentrations at tillering stage with respect to the water seeded treatments (Table S3).

Thioarsenates were observed in all mesocosms of both soils at all seven sampling stages (tillering, stem elongation, booting, flowering, grain filling, dough, and mature stage) under both water and dry seeded treatments (Fig. 2a-d). The contribution of thioarsenates to total As ranged from 0.1% to 19%, on average 4.1%. For comparison, methylated oxyarsenates ranged from below detection limit to 33%, on average 6.5%. Concentrations of inorganic thioarsenates were generally higher (max. 6.4 µg/L or 19% of total As) than those of methylated thioarsenates (max. 1.1 µg/L or 8.2% of total As) in both soils. No clear trend in the proportion of inorganic or methylated thioarsenates was observed over time (Fig. 2a-d). For details on trends in total As pore-water concentrations over time see supporting information, section 2.

Sulfate fertilization significantly decreased total pore-water As concentrations (Fig. 2e, f). All S fertilized mesocosms, including dry seeded Veronica soil, had pore-water As concentrations at or below 20 µg/L already at stem elongation stage. The same faster decrease in As concentrations upon addition of sulfate has been reported before due to stimulation of sulfate-reducing bacteria (SRB), increased sulfide

production, and formation of new Fe minerals [20, 28] (Fig. 1). A decrease due to re-adsorption was, however, mainly observed for inorganic oxyarsenic species, while proportions of inorganic and methylated thioarsenates, as well as methylated oxyarsenates, increased with sulfate fertilization (Fig. 3). Average total thiolation with sulfate addition was 5.9% compared to 2.2% in controls, average methylation was 8.8% compared to 4.3% in controls. Higher proportions of methylated As species upon sulfate addition are in line with previous observations [29]. Similar to the control treatment, there were no significant trends in thiolation or methylation over time (Fig. 2a-d).

Seeding practices did not only impact total As concentrations (with higher concentrations in dry compared to water seeded treatments) but also As thiolation. Both without and with sulfate fertilization, higher percentages were observed in water compared to dry seeded mesocosms due to the longer duration of anaerobic conditions in the former (Fig. 3c, g).

Comparison between the two different soils showed that sulfate fertilization had a stronger impact in Veronica compared to Fornazzo soil. We observed both a stronger decrease in total As concentrations (Fig. 2e, f), as well as a stronger increase in average proportions of methylated oxy- and thioarsenates, in both water and dry seeded treatments, as well as inorganic thioarsenates in dry seeded treatments, for Veronica compared to Fornazzo soil (Fig. 3, Table S4). The exact redox chemistry, especially the role of organic C, remains to be investigated, but we propose that the lower soil C content caused less reducing conditions (reflected in higher redox potentials and less aqueous Fe(II); Table S3) in Veronica soil compared to Fornazzo soil. Thereby, besides efficient removal of As on mixed Fe(II)Fe(III) minerals, more recycling of SRB-produced sulfide to sulfate with formation of zero-valent S and As

thiolation (see also below) was favored, compared to more removal on FeS minerals and less thiolation in Fornazzo soil.

Finally, multivariate regression tree analysis comparing the relative importance of the investigated effects on pore-water As speciation in our mesocosms showed the clearest separation between sulfate and non-sulfate treatments, followed by the differences of the two selected soil types. The different rice growing stages had the least effects on pore-water As speciation (Fig. S7).

Thioarsenate formation potential in soil incubations.

To estimate the potential for thioarsenate formation on a large scale, we conducted anaerobic soil incubation experiments with the two Italian soils plus 31 soils sampled from across China (for coordinates see Table S5a). China is one of the biggest rice cultivation countries. The selected soils cover all major rice production regions in China, with paddy soils located in different climate zones (Fig. S8), developed over different parent material, resulting in different soil types (Table S5a, Fig. S9), and at sites of different geology and geomorphology (Table S5b). The samples cover a wide range of soil pH (4.5 to 9.0), total As contents (2.6 to 38.8 mg/kg), 0.5 M HCl-extractable Fe (30 to 184 mmol/kg), and SOM (14.0 to 104 g/kg) (Table S5c).

After two weeks of incubation, As thiolation was detected in all paddy soils with and without sulfate addition. The proportion of total thioarsenates ranged from 0.1% to 56%, with an average of 9.6% and a median of 4.8% (Fig. S10a). In comparison, the proportion of methylated oxyarsenates ranged from 0.5% to 17%, with an average of 3.1% and a median of 1.8% (Fig. S10e). The dominant individual As species were DTA (> trithioarsenate (TTA) > MTA) and DMDTA (> MMMTA $\geq$ MMDTA > DMMTA)

for inorganic and methylated thioarsenates, respectively (Fig. S11), with different factors controlling their formation.

For inorganic thioarsenates, high absolute concentrations tended to occur at high soil pH and soil zero-valent S contents (Fig. 4a, b, confirmed by Spearman correlation (Table S6) and principal component analysis (Fig. S12)). The pH-dependency of inorganic thioarsenates formation is at first glance surprising. Inorganic thioarsenates are known to transform to oxyarsenic species at low pH [15, 16], but even though soil pH (when oxic) ranged from 4.5 to 9.0, pore-water pH values of all incubations were near-neutral to slightly alkaline (6.9 to 7.9; Fig. S13a) and should not have influenced inorganic thioarsenate (trans)formation. Linear regression analysis showed that the most important predictor for inorganic thioarsenate formation potential in our incubations was soil zero-valent S (weight factor 51%, Fig. 4e, Table S7). Soil zero-valent S increased with soil pH (Fig. S13c), which explains the observed correlation of soil pH and inorganic thioarsenates as an indirect effect through zero-valent S. In most samples, we also detected aqueous zero-valent S (Fig. S13d), but absolute concentrations were more than one order of magnitude lower than those for solid phase zero-valent S, and even in the absence of detectable aqueous zero-valent S, inorganic thioarsenates were observed. The greater impact of solid phase zero-valent S is consistent with previous observations in low-sulfide terrestrial environments where inorganic thioarsenate formation was found to be controlled by reactions with S bound to surfaces of minerals or organic matter [10, 14]. The concentrations of pedogenetic (0.5 M HCl-extractable) Fe had a negative, but relatively low impact on inorganic thioarsenate formation potential (weight factor -6%, Fig. 4e, Table S7), likely because little Fe dissolved at high pH (Fig. S13e).

Methylated thioarsenates showed a completely different behavior. The most important predictor for their formation was the proportion of methylated oxyarsenates (weight factor 46%, Fig. 4e, Table S7). Methylated thio- and oxyarsenates showed a strong positive correlation (Fig. 4d, Table S6). Negative correlation of methylated thioarsenates with soil pH (Fig. 4c, Table S6) suggests that their formation in nature proceeds by nucleophilic attack of reduced S to the As atom which is facilitated at low pH [12]. The higher proportion of methylated oxyarsenates observed at low pH (Fig. S8e) is in line with previous observations in other environments of highest methylation rates at pH 3.5 to 5.5 [30]. An almost even contribution of thio- and oxyarsenates to total methylation (Fig. 4d), as well as the absence of a correlation with zero-valent S (Table S6), suggest that thiolation of methylated species proceeds rapidly and is typically not limited by S supply but mainly by the availability of methylated oxyarsenates (in contrast to inorganic thioarsenates where relatively large excess of S over arsenite is required for thiolation). Examining soil properties, low total soil As concentrations were the best predictor of the potential for a high (thio)methylation contribution to total As (weight factor -40%, Fig. 4e, Table S7). We found that high soil As concentrations only led to increased inorganic As release into pore-water while absolute concentrations of methylated species did not change with increasing total soil As and therefore relative contributions decreased (Fig. S14). Finally, pedogenetic Fe had a stronger negative impact on methylated thioarsenates compared to inorganic thioarsenates (weight factor -27%, Fig. 4e, Table S7), likely because of the higher Fe solubility at low pH (Fig. S13e) where methylated thioarsenates prevailed.

Compared to the strong effects that the different soil properties had on thiolation in our incubation experiments, the effect of sulfate addition was less pronounced. It promoted total thiolation (Fig. S15a) by increasing zero-valent S contents (Fig. S13c,

S15b) and decreasing pore-water Fe concentrations (Fig. S13e) and redox potential (Fig. S13b), but it did not generally change the relative differences in thioarsenate formation potential between different soils. An exception were soils that had very low initial soil zero-valent S contents. Here, sulfate addition led to a strong increase in zero-valent S and total thiolation (Fig. S15b, c). An example was Veronica soil where an increase of zero-valent S from 0.14 to 0.41 mmol/kg compared to a much smaller increase in Fornazzo soil (from 0.34 to 0.39 mmol/kg) might explain the observed stronger increase in total As thiolation in the soil incubations (inorganic thioarsenates from 3.9 to 24%, methylated thioarsenates from 25 to 32%) which is also in line with an observed stronger increase of total thiolation upon sulfate addition in the mesocosm studies (from 1.9 to 6.2%).

Environmental implications

Our combined results from field surveys, mesocosms, and soil incubations reveal thioarsenates as important but previously overlooked and unforeseen contributing species to As biogeochemistry in rice paddies. Thioarsenates form in various paddy soil types, throughout the cropping season, independent of seeding practice, and in quantities comparable to methylated oxyarsenates. Soil pH represented an easy-to-measure parameter indicative for thiolation potential. We suspect that in paddy soils where methylated oxyarsenates have been identified, methylated thioarsenates could have contributed comparable quantities that were, however, not distinguished from the methylated oxyarsenates due to analytical limitations in the current methodologies adopted. Sulfate fertilization promotes thiolation, especially in soils originally low in zero-valent S.

Comparison of our anaerobic soil incubations to mesocosm experiments shows lower proportions of inorganic and especially methylated thioarsenates in the presence of rice plants (Fig. S16). Higher order thiolated inorganic arsenates [15] and MMMTA [31] are known to be oxygen-sensitive, so that root radial oxygen loss might lead to (partial) transformation in the rhizosphere. However, MTA [15] and DMMTA [32] are not oxygen-sensitive. The differences in the proportion of thioarsenates between incubations and mesocosms might therefore point towards their preferential uptake. So far, uptake of thioarsenates and their efficient root-shoot translocation has only been shown in hydroponic cultures using high concentrations of pure thioarsenate standards [33, 34] and only one thioarsenate species (DMMTA) has been discovered in commercial rice grains by chance during an enzymatic extraction [35]. Now that we deliver compelling support of the widespread presence of inorganic and methylated thioarsenates in paddy soil pore-waters, further transfer of methods and experiments from laboratory to field scale is required. Whether thiolation finally is boon or bane for rice safety remains to be investigated.

Methods

Aqueous As species preservation and analysis

Arsenic speciation throughout the study was done using ion chromatography (IC, Dionex ICS-3000; AG/AS16 IonPac column, 4 mm, eluent gradient 2.5−100 mM NaOH at a flow rate of 1.2 mL/min) coupled to inductively coupled plasma-mass spectrometry (ICP-MS, XSeries2, Thermo-Fisher) at Bayreuth University. Retention times of the As species were verified by comparison with commercial standards (arsenite ($NaAsO_2$, Fluka), arsenate ($Na_2HAsO_4 \times 7H_2O$, Fluka), MMA ($CH_3AsNa_2O_3 \times 6H_2O$, Supelco), DMA ($C_2H_6AsNaO_2 \times 3H_2O$, Sigma-Aldrich)), standards synthesized according to previously published methods (DMMTA (purity 67%; 28% DMDTA, 5% DMA) and MMMTA (purity 96%; 1% MMA, 3% MMDTA) [34], MTA (purity of 98.5%; 0.5% arsenite, 1% arsenate) [33]) or by comparison with previously published retention times (MMDTA, DMDTA, DTA, TTA) [11].

For our initial field survey (see supporting information section 1) we used sample flash-freezing, a preservation method that we previously employed successfully in other aquatic environments [10, 13, 14]. In contrast to sample acidification, this method revealed the occurrence of thioarsenates. However, we observed that As recoveries (calculated as the sum of all detected As species in flash-frozen samples versus total As measured in oxidized and HNO_3-acidified samples) were generally below 50%, in many cases even below 10% (Fig. S4), especially at Fe concentrations > 0.5 mM due to Fe (oxyhydr)oxide precipitation and As co-precipitation and sorption. The low recoveries prompted us to adapt the sample preservation and analysis method. Since acidification could not be used to keep Fe in solution because it changes thioarsenate speciation and could lead to AsS mineral precipitation [36], we tested different Fe chelating agents. In pre-tests, paddy soil solutions derived from

anaerobic incubations were preserved with different pH-neutralized chelating agents such as EDTA (ethylenediaminetetraacetic acid disodium salt solution, Sigma–Aldrich), deferoxamine mesylate salt (Sigma-Aldrich), and DTPA (diethylenetriamine-pentaacetic acid pentasodium salt, Sigma-Aldrich). Highest As species recoveries were observed when using DTPA, an octadentate ligand which can completely sequester Fe [37, 38]. The better performance compared to EDTA, for which we previously reported accelerated oxidation of arsenite and some thioarsenate artefact formation [39], might be attributed to the fact that Fe^{II}-DTPA complexes are significantly less oxygen-sensitive than Fe^{II}-EDTA complexes[40]. Based on expected high aqueous Fe concentrations in the sampled paddy soil pore-waters (measured values up to 6.9 mM in samples from China, see section 4), we used 10 mM DTPA, neutralized to pH 7.5, for Fe-complexation.

For a representative paddy soil pore-water matrix (“model pore-water”) for method development, we used pore-waters extracted from anaerobic incubations of paddy soil from Fornazzo (for details on soil properties see section 3, description of mesocosms). To address the effect of DTPA on As species retention times, peak shape, and species resolution, one week old model pore-water was spiked with 100 µg/L of different As species standards and 10 mM DTPA was added for sample preservation. DTPA had a significant effect on peak shapes and retention times, especially for the species with short retention times (Fig. S17). The DMA peak that eluted after 297 s in the absence of DTPA was shifted to the dead volume (142 s, Fig. S17a). DMMTA and DMDTA were partially retained at their original retention times (376 and 446 s) but peaks became wide and small and part of the As was lost in a high baseline background from 150 to 350 s (Fig. S17b). The same change in peak shape and total As loss was observed for arsenite (original retention time at 406 s; Fig. S17c). Mixes of arsenite, DMA, and DMMTA also showed that species resolution

between arsenite and DMMTA was lost in the presence of DTPA (Fig. S17d). MMMTA and arsenate were less affected but peak splitting (Fig. S17e) and peak fronting (Fig. S17f), respectively, were observed in the presence of DTPA as well.

Since we could not reduce the DTPA concentration because of the expected Fe concentrations but needed to decrease the negative effects of DTPA on peak separation, we tested 10-fold dilution with deionized water of a fresh model pore-water sample without As spikes after addition of 10 mM DTPA (bringing DTPA concentrations down to 1 mM, but also diluting Fe, As, etc. 10-fold). The 1:10 sample dilution increased peak separation and largely avoided As elution in the dead volume (Fig. S18) but some peaks were close to or below detection limit. Adding 2.4% methanol to the 2.5-100 mM NaOH gradient eluent in the IC enhanced signal intensities of all peaks, except for arsenite, by a factor of 2 to 10 (Fig. S18). A slight decrease in retention times and some arsenate fronting was observed, but all peaks could be identified and little As was lost in the dead volume.

For a quantitative evaluation we spiked the fresh model pore-water sample with a mixed standard of 1 µg/L of DMA, DMMTA, arsenite, MMA, MMMTA, and arsenate. Comparing preservation in 10 mM DTPA in deionized water vs. model pore-water matrix (analyzed 1:5 and 1:10 diluted), showed that the pore-water matrix itself had a minor effect on peak shifting compared to the influence of DTPA (Fig. S19). A dilution of 1:5 resulted in peak broadening for DMA and DMMTA but no additional As loss. Quantitatively, the results of 1:10 or 1:5 dilution were comparable (Table S8). Measured total As concentration in HNO_3 for that sample was 14.3 µg/L and recovery from speciation analysis for the 1:10 and 1:5 dilution with 76% and 77%, respectively, was good. Species with concentrations of 0.28 and 0.15 µg/L (equivalent to 2.5 and 1% of total As) could clearly be identified in the 1:10 and 1:5 dilutions, respectively.

Three commercial standards were routinely used for calibration (arsenate dibasic-heptahydrate, disodium methyl arsonate hexahydrate, dimethylarsinic acid in 2 mM DTPA). No significant differences were observed between using an average calibration of the three commercial standards or calibrating each species individually using the calibration standard which was closest in retention time. Arsenite was not used for calibration because in deionized water we observed transformation of arsenite in the presence of DTPA (Fig. S20). The arsenite transformation product eluted at the retention time of arsenate but with significant peak fronting. Whether the species really is arsenate (obtained from arsenite oxidation) or an As(III)- or As(V)-DTPA complex is currently unclear. In spiked natural samples, we did not observe this arsenite transformation.

The final protocol for As speciation that was applied for the mesocosm and incubation experiments described in the following is summarized as follows. Samples were filtered, preserved in 10 mM DTPA, flash-frozen on dry ice, and stored at -20 °C. Prior to analysis, frozen samples were thawed under anoxic atmosphere inside a glovebox (COY, N_2/H_2 95/5% (v/v)) at room temperature. Samples were diluted 1:5 with deionized water and analyzed with a 2.5-100 mM NaOH gradient containing 2.4% methanol.

We are aware that sample dilution might transform higher thiolated As species such as DMDTA, MMDTA, DTA, or TTA as reported previously [41] and that we may therefore underestimate the extent of As thiolation. Further, recoveries generally were >80%, which is good considering that we calculate the sum of up to 11 species, but could still indicate a loss of As species by Fe scavenging. Therefore, where species proportions are reported in %, the reference is not the sum of species, but always total As from a sample preserved with 0.5% H_2O_2 and 0.8% HNO_3 as an

independent measurement. The reported % values are therefore minimum values if a species is not affected at all by Fe scavenging. If thiolated species are scavenged by Fe similar to arsenite and arsenate we may further slightly underestimate their importance with the currently available analytical methods. Despite some remaining shortcomings, the developed DTPA-method is the current best compromise, given the complexity of the paddy soil pore-water samples which are rich in organic carbon, contain high Fe that is prone to oxidation (so mere flash-freezing does not work) and As-complexed sulfide that is prone to precipitation at low pH (so acidification does not work) plus relatively low concentrations of As. The method enabled us to provide the so far most complete aqueous As speciation data for paddy soil pore-waters.

Mesocosm rice cultivation

For mesocosm experiments, we selected two paddy soils characterized by highest proportions of thiolation in pore-water during our field survey in August 2016, Veronica (E 8°53′48″, N 45°10′39″; Eutric Gleysol) and Fornazzo (E 8°57′50″, N 45°13′54″; Umbric Gleysol) (Table S1, S2). A large batch of dry soil material was collected from the plow layer of the two fields in March 2017 and transported to the Rice Research Centre Ente Nazionale Risi (ENR) in Castello d'Agogna (Pavia, Italy) where we set up the mesocosms. For basic soil characterization, soil pH (measured in 2.5 mL 0.1 M $CaCl_2$ solution with 1 g soil), 0.5 M HCl-extractable Fe, total C and N (CHN analyzer), and total S (determination by ICP-MS after microwave digestion in aqua regia) were determined.

Twenty-four plastic containers (0.82 m^2) were installed open air at the property of ENR. A nylon mesh roof top protected the setup from birds or hail. Each container was filled with approximately 30 cm of gravel with a size of 2-5 cm in diameter,

overlaid by approximately 20 cm of soil. Twelve containers each were filled with the two different paddy soil types (Fig. S5). The soil layers were mixed with 5 t/ha equivalent rice straw according to the common rice straw returning practice in this region. The rice straw was cut into pieces of approximately 20 cm length before mixing it with the soil. Six containers of each paddy soil type were either dry or water seeded. Water seeded soils were first fertilized with 100 kg N/ha and flooded on May, 16th (Fig. S6) before sowing with pre-germinated rice seeds (*Oryza sativa* L. cv. Selenio) the following day. Dry seeded soils were fertilized with 100 kg N/ha and sown on May, 17th (Fig. S6). Planted seeds germinated within 10 days. Soils were kept moist until tillering stage (June, 6th) and subsequently flooded. All mesocosms were manually thinned to 340 rice plants per container. Irrigation water (characteristics see Table S9) was supplied with a garden hose for both dry and water seeded treatments, to maintain a standing water level of approximately 10 cm depth during the cropping season. In addition to basal fertilization, N-, P-, or K-fertilizers were applied in form of urea, triple superphosphate, and potassium chloride as solid salts at tillering, stem elongation and booting stages (Fig. S6). Three containers of each soil and seeding practice were additionally fertilized with sulfate fertilizer, the other three containers did not receive sulfate (control treatments). Sulfate was applied as ammonium sulfate and potassium sulfate, while equivalent amounts of urea and potassium chloride were used in the control treatment.

Sampling was done at seven rice growing stages, namely tillering stage (June, 14th), stem elongation stage (July, 4th), booting stage (July, 18th), flowering stage (August, 1th), grain filling stage (August, 8th), dough stage (August, 22th), and mature stage (September, 13th) (Fig. S6). Pore-water was extracted by micro rhizon samplers (Rhizon MOM, Rhizosphere Research Products, The Netherlands) inserted about 3-4 cm deep into the paddy soil and connected to 100 mL evacuated glass bottles. The

bottles were prepared prior to sampling by purging them with argon (purity > 99.9%) for 15 min, sealing them with a butyl rubber septum and then evacuating them to negative atmospheric pressure of ~900 mbar. Sampling took on average 40 minutes. An aliquot of pore-water was preserved in 10 mM DTPA, flash-frozen on dry ice, and stored at -20°C until analysis. Non-stable chemical parameters (pH, redox potential) were measured immediately on-site. Samples for dissolved organic carbon (DOC) and dissolved inorganic carbon (DIC) were kept anoxic, in the dark at 4°C, and analyzed the following day at the University of Turin (VarioTOC, Elementar, Hanau, Germany). Information on pH, E_H, conductivity, DIC, DOC, Fe(II), and total As can be found in Table S3.

Soil sampling and anaerobic incubations

Paddy soil samples were collected from the cultivated horizon of 31 different paddy fields across China, which represent the main rice production regions in 18 different Chinese provinces. The geographic origins covered an area from 22.5° to 47.2° N and 98.4° to 131.6° E, spanning climate zones from sub-tropical monsoon climate (23 soils) to temperate continental climate (1 soil) and temperate monsoon climate (7 soils) (Fig. S8). Based on the Chinese soil taxonomic classification, all paddy soils are classified as Stagnic Anthrosols with both a hydragric epipedon (including cultivated horizon and plowpan) and a hydragric horizon. Those paddy soils represent three out of four key groups of Stagnic Anthrosols, namely Fe-accumuli- (15), Fe-leachi-(8), and Hapli- (8) Stagnic Anthrosols (Fig. S9). Detailed information regarding sampling site coordinates, soil classification, parent material, geology, geomorphology, and climate zone can be found in Table S5a, 5b. Twenty-nine out of the 31 paddy fields had As concentrations below the Chinese risk screening values

for contamination of agricultural land (30 mg/kg when pH ≤ 6.5 [42]), and are thus considered to represent the natural background. Only two soils namely Guangxi-Nanning (CH2, 34.2 mg/kg) and Jiangxi-Ganzhou (CH6, 38.8 mg/kg) exceeded the Chinese risk screening values for paddy soil. We intentionally focused on non-contaminated paddy soils having background As concentrations because of the wider implications linked with human exposure, with respect to the less ubiquitous anthropogenically-contaminated sites (e.g. only 2.7% of paddy soils in China according to a recent survey [43]), that often have rather specific biogeochemistries that greatly depend on contamination source and type.

Selected soil properties, including pH, 0.5 M HCl-extractable Fe, SOM, CEC, clay content, total As and other chalcophile metals (Cd, Pb, Cu and Zn), and soil zero-valent S content were analyzed by standard methods [44, 45, 46]. All soils were air-dried and sieved to < 2 mm before analysis and incubation.

For incubation, 10 g dry soil was suspended in 20 mL of 2.5 mM glucose solution without (control, no S) or with 1.5 mM K_2SO_4 (3 mmol/kg sulfate, S) in a glovebox (N_2/H_2 95/5% (v/v)). The vials were incubated anaerobically, at room temperature and in the dark for 14 days. This duration was assumed from pre-experiments and literature [47] to be sufficient for microbial growth to reach a steady state. For sampling, soil suspensions were centrifuged and filtered (0.2 µm). Aqueous phase parameters (pH, redox potential, dissolved free sulfide and aqueous zero-valent S, total As) were measured as described above. Another aliquot was preserved in 10 mM DTPA, flash-frozen on dry-ice, and stored at -20 °C for As speciation analysis. Aqueous total Fe was measured immediately by the ferrozine test [48]. Soil for solid phase zero-valent S extraction was first freeze-dried (EDWARDS Modyla & Vacuum oven Heraeus), then extracted with chloroform (10 mg soil + 700 µL chloroform) and analyzed by

HPLC [49]. Thus, soil-bound zero-valent S in our study is operationally defined as chloroform-extractable, reduced inorganic S.

Statistical analyses

All statistical analyses were performed via R statistical computing environment. Spearman's correlation was calculated using the "Hmisc" package. Principal component analysis of As species (DMA, MMA, DMDTA, MMDTA, MMMTA, DMMTA, MTA, DTA, and TTA) in the batch incubations was calculated using the "vegan" package. Multiple linear regression (MLR) analysis between inorganic and methylated thioarsenates (%), respectively, and soil physical and chemical properties (soil pH, total zero-valent S, total soil As, 0.5 M HCl-extractable Fe, CEC, SOM, clay content, and soil chalcophile metals (sum of Cd, Pb, Cu. and Zn)) was done using "MASS" package (with default parameters). For methylated thioarsenates two models were calculated, one with, a second without considering methylated oxyarsenates. Relative importance of variables in multiple regression was calculated using the "relaimpo" package (type = "lmg") [50]. Residuals were checked for normal distribution, which is a prerequisite for multiple linear regression. Multivariate regression tree analyses were done using the "mvpart" package (with default parameters) [51].

Reference

1. Stone R. Arsenic and paddy rice: A neglected cancer risk? *Science* 2008, **321**(5886)**:** 184-185.

2. Ma JF, Yamaji N, Mitani N, Xu X-Y, Su Y-H, McGrath SP*, et al.* Transporters of arsenite in rice and their role in arsenic accumulation in rice grain. *Proceedings of the National Academy of Sciences* 2008, **105**(29)**:** 9931-9935.

3. Wang P, Zhang W, Mao C, Xu G, Zhao F-J. The role of OsPT8 in arsenate uptake and varietal difference in arsenate tolerance in rice. *Journal of Experimental Botany* 2016, **67**(21)**:** 6051-6059.

4. Ye Y, Li P, Xu T, Zeng L, Cheng D, Yang M*, et al.* OsPT4 contributes to arsenate uptake and transport in rice. *Frontiers in Plant Science* 2017, **8**(2197).

5. Xu XY, McGrath SP, Meharg AA, Zhao FJ. Growing rice aerobically markedly decreases arsenic accumulation. *Environmental Science & Technology* 2008, **42**(15)**:** 5574-5579.

6. Jia Y, Huang H, Zhong M, Wang F-H, Zhang L-M, Zhu Y-G. Microbial arsenic methylation in soil and rice rhizosphere. *Environmental Science & Technology* 2013, **47**(7)**:** 3141-3148.

7. Lomax C, Liu WJ, Wu LY, Xue K, Xiong JB, Zhou JZ*, et al.* Methylated arsenic species in plants originate from soil microorganisms. *New Phytologist* 2012, **193**(3)**:** 665-672.

8. Zhao F-J, Zhu Y-G, Meharg AA. Methylated arsenic species in rice: geographical variation, origin, and uptake mechanisms. *Environmental Science & Technology* 2013, **47**(9)**:** 3957-3966.

9. Meharg AA, Zhao F-J. Biogeochemistry of arsenic in paddy environments. *Arsenic & Rice*. Springer, 2012, pp 71-101.

10. Besold J, Biswas A, Suess E, Scheinost AC, Rossberg A, Mikutta C*, et al.* Monothioarsenate Transformation Kinetics Determining Arsenic Sequestration by Sulfhydryl Groups of Peat. *Environmental Science & Technology* 2018, **52**(13)**:** 7317-7326.

11. Wallschläger D, London J. Determination of methylated arsenic-sulfur compounds in groundwater. *Environmental Science & Technology* 2007, **42**(1)**:** 228-234.

12. Conklin SD, Fricke MW, Creed PA, Creed JT. Investigation of the pH effects on the formation of methylated thio-arsenicals, and the effects of pH and temperature on their stability. *J Anal Atom Spectrom* 2008, **23**(5)**:** 711-716.

13. Planer-Friedrich B, London J, McCleskey RB, Nordstrom DK, Wallschläger D. Thioarsenates in geothermal waters of Yellowstone National Park: determination, preservation, and geochemical importance. *Environmental Science & Technology* 2007, **41**(15)**:** 5245-5251.

14. Planer-Friedrich B, Schaller J, Wismeth F, Mehlhorn J, Hug SJ. Monothioarsenate occurrence in bangladesh groundwater and its removal by ferrous and zero-valent iron technologies. *Environmental Science & Technology* 2018, **52**(10)**:** 5931-5939.

15. Planer-Friedrich B, Wallschläger D. A critical investigation of hydride generation-based arsenic speciation in sulfidic waters. *Environmental Science & Technology* 2009, **43:** 5007-5013.

16. Smieja JA, Wilkin RT. Preservation of sulfidic waters containing dissolved As(III). *Journal of Environmental Monitoring* 2003, **5**(6)**:** 913-916.

17. Kogel-Knabner I, Amelung W, Cao ZH, Fiedler S, Frenzel P, Jahn R*, et al.* Biogeochemistry of paddy soils. *Geoderma* 2010, **157**(1-2)**:** 1-14.

18. Wind T, Conrad R. Localization of sulfate reduction in planted and unplanted rice field soil. *Biogeochemistry* 1997, **37**(3)**:** 253-278.

19. Ayotade KA. Kinetics and reactions of hydrogen sulphide in solution of flooded rice soils. *Plant and Soil* 1977, **46**(2)**:** 381-389.

20. Saalfield SL, Bostick BC. Changes in Iron, Sulfur, and Arsenic Speciation Associated with Bacterial Sulfate Reduction in Ferrihydrite-Rich Systems. *Environmental Science & Technology* 2009, **43**(23)**:** 8787-8793.

21. Burton ED, Johnston SG, Kocar BD. Arsenic mobility during flooding of contaminated soil: the effect of microbial sulfate reduction. *Environmental Science & Technology* 2014, **48**(23)**:** 13660-13667.

22. Xu LY, Wu X, Wang SF, Yuan ZD, Xiao F, Ming Y*, et al.* Speciation change and redistribution of arsenic in soil under anaerobic microbial activities. *Journal of Hazardous Materials* 2016, **301:** 538-546.

23. Crusciol CAC, Nascente AS, Soratto RP, Rosolem CA. Upland rice growth and mineral nutrition as affected by cultivars and sulfur availability. *Soil Science Society of America Journal* 2013, **77**(1)**:** 328-335.

24. Schütz H, Holzapfel-Pschorn A, Conrad R, Rennenberg H, Seiler W. A 3-year continuous record on the influence of daytime, season, and fertilizer treatment on methane emission rates from an Italian rice paddy. *Journal of Geophysical Research: Atmospheres* 1989, **94**(D13)**:** 16405-16416.

25. Minamikawa K, Sakai N, Hayashi H. The effects of ammonium sulfate application on methane emission and soil carbon content of a paddy field in Japan. *Agriculture, Ecosystems & Environment* 2005, **107**(4)**:** 371-379.

26. Fan J, Xia X, Hu Z, Ziadi N, Liu C. Excessive sulfur supply reduces arsenic accumulation in brown rice. *Plant, Soil and Environment* 2013, **59**(4)**:** 169-174.

27. Zhang J, Zhao C-Y, Liu J, Song R, Du Y-X, Li J-Z*, et al.* Influence of sulfur on transcription of genes involved in arsenic accumulation in rice grains. *Plant Molecular Biology Reporter* 2016, **34**(3)**:** 556-565.

28. Jia Y, Bao P. Arsenic bioavailability to rice plant in paddy soil: influence of microbial sulfate reduction. *Journal of Soils and Sediments* 2015, **15**(9)**:** 1960-1967.

29. Zeng X, Jiang Y, Fan X, Chao S, Yang Y, Liu J*, et al.* Effects of sulfate application on inhibiting accumulation and alleviating toxicity of arsenic in panax notoginseng grown in arsenic-polluted soil. *Water, Air, & Soil Pollution* 2016, **227**(5)**:** 148.

30. Baker M, Inniss W, Mayfield C, Wong P, Chau Y. Effect of pH on the methylation of mercury and arsenic by sediment microorganisms. *Environmental Technology Letters* 1983, **4**(2)**:** 89-100.

31. Cullen WR, Liu Q, Lu X, McKnight-Whitford A, Peng H, Popowich A*, et al.* Methylated and thiolated arsenic species for environmental and health research — A review on synthesis and characterization. *Journal of Environmental Sciences* 2016, **49:** 7-27.

32. Kim Y-T, Lee H, Yoon H-O, Woo NC. Kinetics of dimethylated thioarsenicals and the formation of highly toxic dimethylmonothioarsinic acid in environment. *Environmental Science & Technology* 2016.

33. Kerl CF, Rafferty C, Clemens S, Planer-Friedrich B. Monothioarsenate uptake, transformation, and translocation in rice plants. *Environmental Science & Technology* 2018, **52**(16)**:** 9154-9161.

34. Kerl CF, Schindele RA, Brüggenwirth L, Colina Blanco AE, Rafferty C, Clemens S*, et al.* Methylated thioarsenates and monothioarsenate differ in uptake, transformation, and contribution to total arsenic translocation in rice plants. *Environmental Science & Technology* 2019, **53**(10)**:** 5787-5796.

35. Ackerman AH, Creed PA, Parks AN, Fricke MW, Schwegel CA, Creed JT*, et al.* Comparison of a chemical and enzymatic extraction of arsenic from rice and an assessment of the arsenic absorption from contaminated water by cooked rice. *Environmental Science & Technology* 2005, **39**(14)**:** 5241-5246.

36. Planer-Friedrich B, Wallschläger D. A critical investigation of hydride generation-based arsenic speciation in sulfidic waters. *Environmental Science & Technology* 2009, **43**(13)**:** 5007-5013.

37. Tang L, Yang J, Shen X. Effects of additional iron-chelators on Fe 2+-initiated lipid peroxidation: Evidence to support the Fe 2+… Fe 3+ complex as the initiator. *Journal of Inorganic Biochemistry* 1997, **68**(4)**:** 265-272.

38. Colman BP. Understanding and eliminating iron interference in colorimetric nitrate and nitrite analysis. *Environmental Monitoring and Assessment* 2010, **165**(1-4)**:** 633-641.

39. Suess E, Wallschläger D, Planer-Friedrich B. Stabilization of thioarsenates in iron-rich waters. *Chemosphere* 2011, **83**(11)**:** 1524-1531.

40. Zang V, Van Eldik R. Kinetics and mechanism of the autoxidation of iron (II) induced through chelation by ethylenediaminetetraacetate and related ligands. *Inorganic Chemistry* 1990, **29**(9)**:** 1705-1711.

41. Suess E, Scheinost AC, Bostick BC, Merkel BJ, Wallschlaeger D, Planer-Friedrich B. Discrimination of thioarsenites and thioarsenates by X-ray absorption spectroscopy. *Analytical Chemistry* 2009, **81**(20)**:** 8318-8326.

42. The Ministry of Ecology and Environment. Soil Environment Quality Risk Control Standard for Soil Contamination of Agriculture Land *GB 15618-2018* 2018.

43. Zhao F-J, Ma Y, Zhu Y-G, Tang Z, McGrath SP. Soil contamination in China: current status and mitigation strategies. *Environmental Science & Technology* 2014, **49**(2)**:** 750-759.

44. Ratering S, Schnell S. Localization of iron-reducing activity in paddy soilby profile studies. *Biogeochemistry* 2000, **48**(3)**:** 341-365.

45. Stroud JL, Khan MA, Norton GJ, Islam MR, Dasgupta T, Zhu Y-G*, et al.* Assessing the labile arsenic pool in contaminated paddy soils by isotopic dilution techniques and simple extractions. *Environmental Science & Technology* 2011, **45**(10)**:** 4262-4269.

46. Zhang S-Y, Zhao F-J, Sun G-X, Su J-Q, Yang X-R, Li H*, et al.* Diversity and abundance of arsenic biotransformation genes in paddy soils from Southern China. *Environmental Science & Technology* 2015, **49**(7)**:** 4138-4146.

47. Zhao F-J, Harris E, Yan J, Ma J, Wu L, Liu W*, et al.* Arsenic methylation in soils and its relationship with microbial arsM abundance and diversity, and As speciation in rice. *Environmental Science & Technology* 2013, **47**(13)**:** 7147-7154.

48. Stookey LL. Ferrozine - A new spectrophotometric reagent for iron. *Analytical chemistry* 1970, **42**(7)**:** 779-781.

49. Lohmayer R, Kappler A, Lösekann-Behrens T, Planer-Friedrich B. Role of sulfur species as redox partners and electron shuttles for ferrihydrite reduction by Sulfurospirillum deleyianum. *Applied and Environmental Microbiology* 2014**:** AEM. 04220-04213.

50. Grömping U. Relative importance for linear regression in R: the package relaimpo. *Journal of Statistical Software* 2006, **17**(1)**:** 1-27.

51. De'Ath G. Multivariate regression trees: a new technique for modeling species-environment relationships. *Ecology* 2002, **83**(4)**:** 1105-1117.

Corresponding Author

Correspondence and requests for materials should be addressed to Britta Planer-Friedrich (b.planer-friedrich@uni-bayreuth.de)

Acknowledgements

We acknowledge financial support for a Ph.D. stipend to Jiajia Wang from the China Scholarship Council (CSC), mobility grants within the Bavarian Funding Programme for travels to France (BFHZ FK-40-15), Italy (BayIntAn2016), China (BayCHINA2018), as well as from the National Key Research and Development Project of China (2016YFE0106400) and the National Natural Science Foundation of China (41325003) for paddy soils survey, sampling and determination in China. We acknowledge data support from the Soil Data Center, National Earth System Science Data Sharing Service Infrastructure, National Science & Technology Infrastructure of China (http://soil.geodata.cn) and Ente Regionale per i Servizi all'Agricoltura e alle Foreste – Regione Lombardia of Italy (https://www.ersaf.lombardia.it/). We are indebted to the staff at the Rice Research Centre in Castello d'Agogna (Pavia, Italy) for help with soil sampling and mesocosm rice cultivation, including Sergio Feccia, Fabio Mazza, Umberto Rolla, Eleonora Miniotti, Gianluca Beltarre, Angela Iuzzolino, Francesca Bonassi, Luca Pizzin, Daniele Tenni, Andrea Zanellato, Federico Massara,

Edoardo Magnani, Gianluca Bertone, and Massimo Zini. We thank Cyrille Thomas and Arnaud Boisnard from the Centre Français du Riz (Arles, Italy) for assistance with soil sampling in France. We are grateful to Michael T.F. Wagner, Cristina Lerda, Stefan Will, José Miguel Leon, Johannes Besold, Laura Wegner and Shuai Zhang for help with field sampling and laboratory assistance, to Yuying Yang for help with map design, and to Judith Mehlhorn for help with statistical analyses.

Additional information

Supplementary information is available ###.

Author contributions

JW initiated DTPA method development, conceived and performed all mesocosm and incubation experiments including analyses, evaluated the results and contributed to manuscript preparation, CK contributed to field survey, sample analyses, data evaluation, and manuscript preparation, LB contributed to DTPA method development, PH & LW initiated the Chinese soil survey and advised on incubation experiments, PH, TM, GW & LW sampled and characterized the Chinese soils, MR assisted in design, setup and operation of mesocosms and sample collection, MM & DSP assisted in analyses of aqueous parameters from mesocosms, MM contributed to field survey and data discussion, BPF initiated and supervised the project, carried out the field survey, conceived experiments, and wrote the manuscript; all authors contributed to revising the manuscript.

Competing financial interests

The authors declare no competing financial interests.

Figures

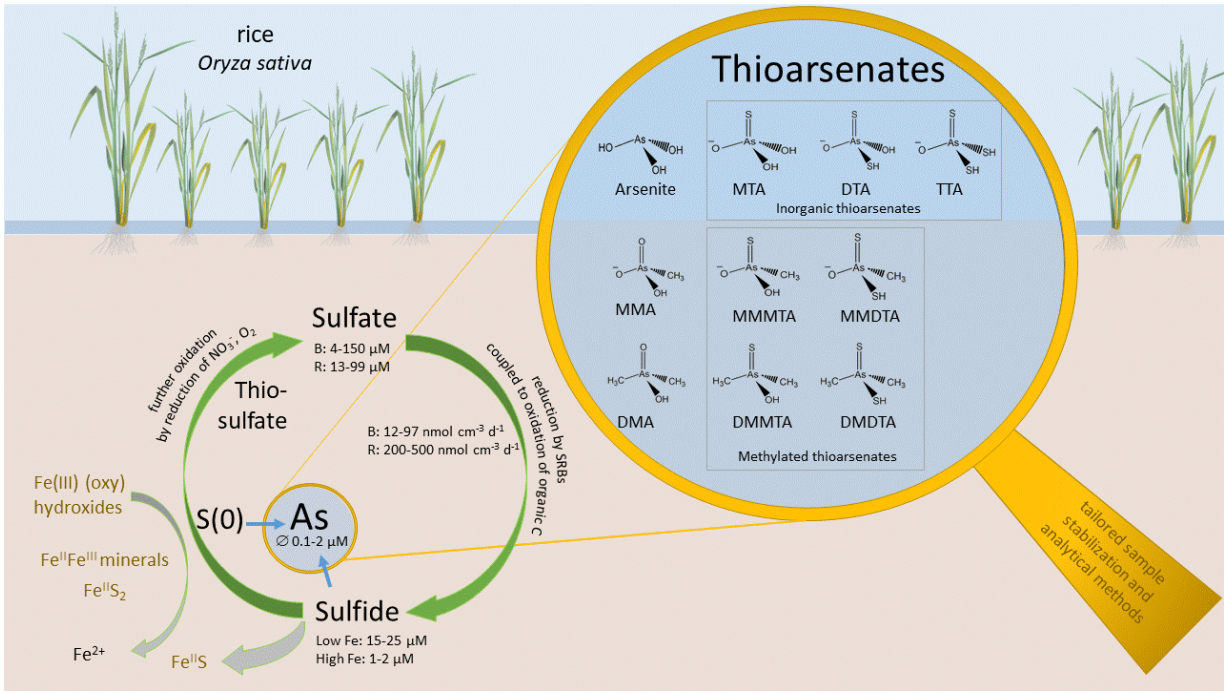

Figure 1 | Conceptual model for the formation of thioarsenates in paddy soils coupled to a cryptic S cycle. Low but continuously replenished concentrations of sulfide and zero-valent sulfur [S(0)] lead to As thiolation instead of or besides As scavenging by newly formed mixed $Fe^{II}Fe^{III}$ minerals and pyrite (FeS_2) or, at excess sulfide, mackinawite (FeS) and AsS; concentrations and rate numbers (taken from references [26] and [27]) are displayed to present typical quantities and extents of sulfate reduction rates (B = bulk soil, R = rhizosphere, SRB = sulfate-reducing bacteria): MTA = monothioarsenate, DTA = dithioarsenate, TTA = trithioarsenate, MMA = monomethylarsenate, MMMTA = monomethylmonothioarsenate, MMDTA = monomethyldithioarsenate, DMA = dimethylarsenate, DMMTA = dimethylmonothioarsenate, DMDTA = dimethyldithioarsenate.

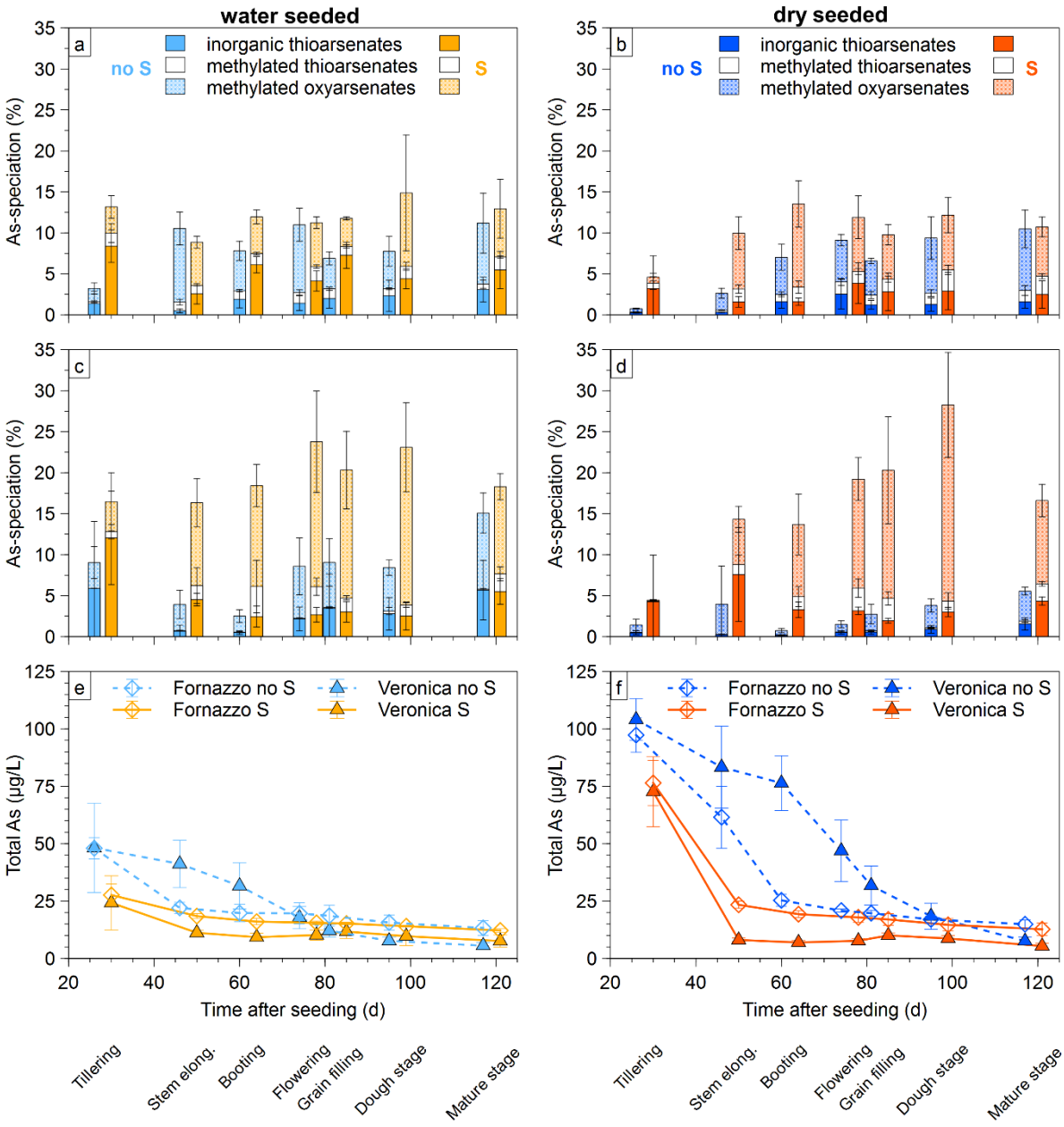

Figure 2 | Pore-water As thiolation, methylation, and total As concentrations over time during rice cultivation. a) Fornazzo soil, water seeded, b) Fornazzo soil, dry seeded, c) Veronica soil, water seeded, d) Veronica soil, dry seeded; blue colors refer to control treatments (no S), orange-red colors to sulfate addition (S); percentages refer to proportion of total As; e, f)

total As concentrations for the two soils with and without sulfate addition; standard deviation reflects results from 3 mesocosms (n=3)

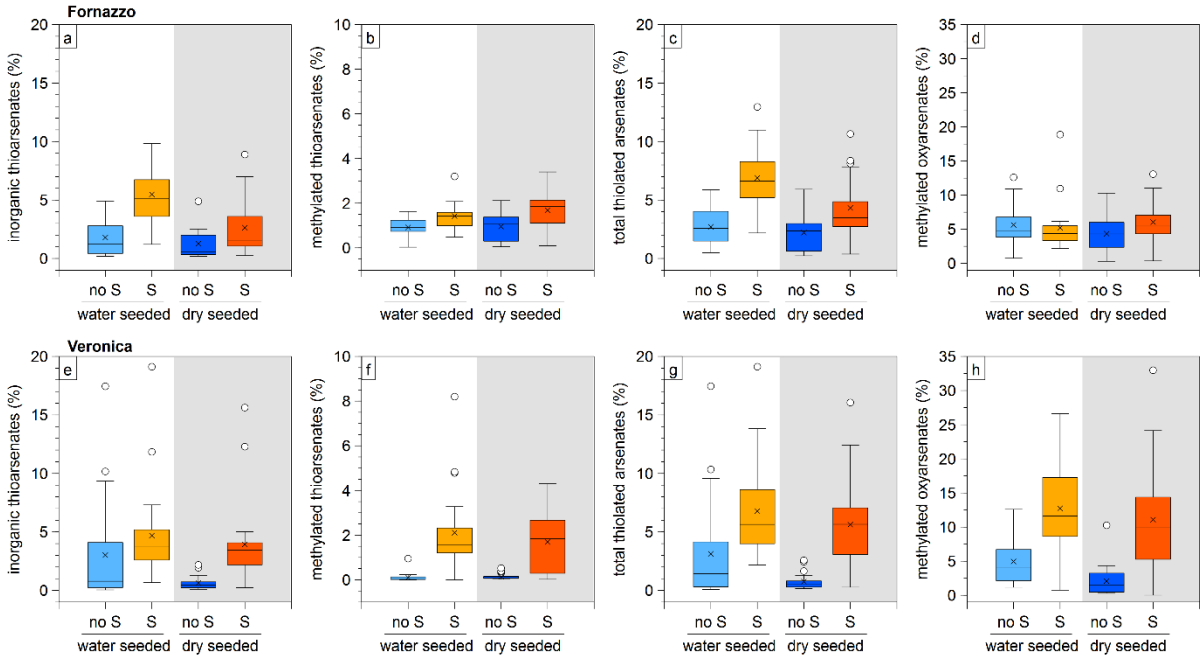

Figure 3 | Proportions of inorganic, methylated, and total thioarsenates as well as methylated oxyarsenates integrated over time. a, e) inorganic thioarsenates, b, f) methylated thioarsenates, c, g) total thioarsenates, d, h) methylated oxyarsenates integrated over all sampling times for Fornazzo and Veronica soils, respectively, water seeded (left side of each graph) and dry seeded (right, shaded side) treatment, blue colors refer to control treatments (no S), orange-red colors to sulfate addition (S); percentages refer to proportion of total As, boxplots: line: median; cross: mean; box: interquartile range; whiskers: 1.5 interquartile range; data from 3 mesocosms over 7 times (n=21)

.

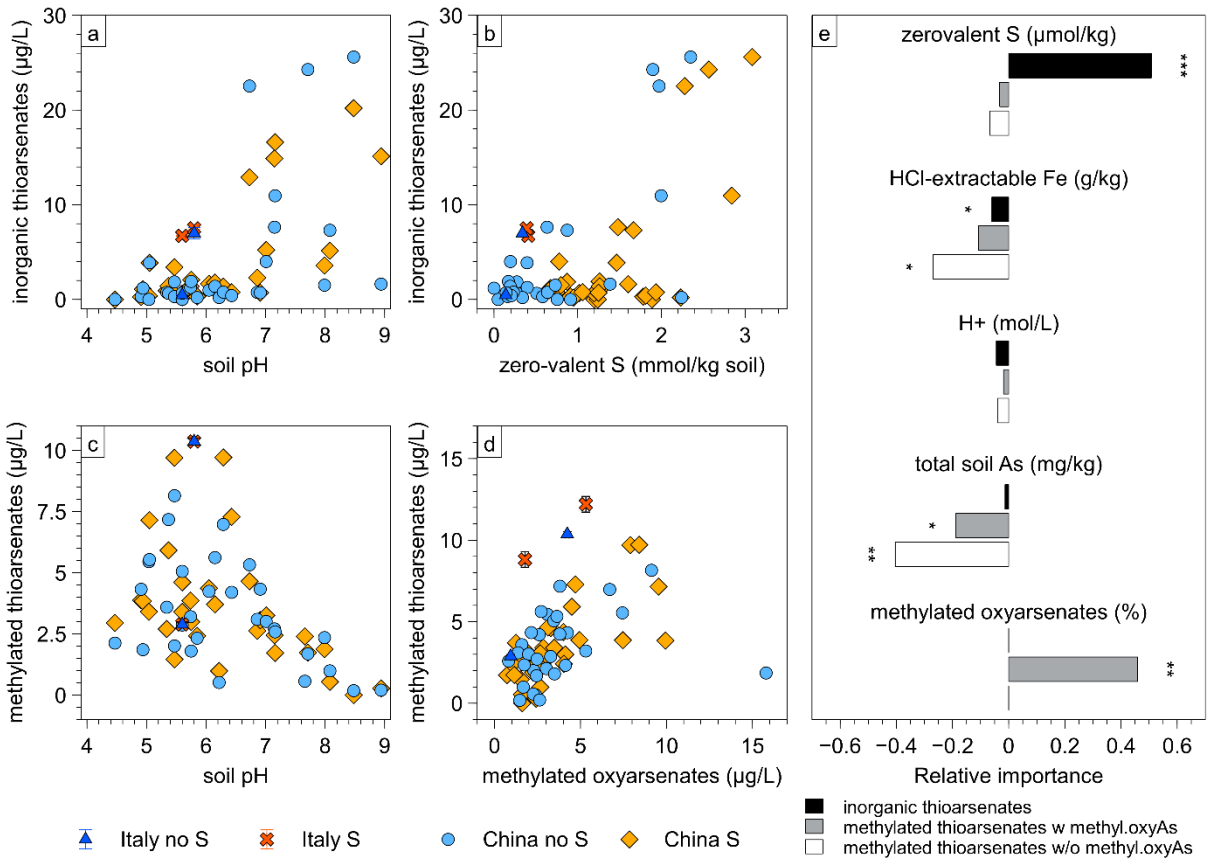

Figure 4 | Parameters that determine occurrence of inorganic and methylated thioarsenates in anaerobic soil incubations. Paddy soils were from Italy (2; experimental triplicates) and China (31, single experiments). a) concentrations of inorganic thioarsenates in relation to soil pH and b) solid phase zero-valent S, c) concentrations of methylated thioarsenates in relation to soil pH and d) methylated oxyarsenates; blue colors refer to control treatments (no S), orange-red colors to sulfate addition (S); e) linear regression analysis showing relative importance of selected soil parameters in control treatments on proportion of inorganic and methylated thioarsenates (with and without considering methylated oxyarsenates) (for complete list of soil parameters considered and data for sulfate addition see Table S7)

Supporting information

Thiolated arsenic species observed in rice paddy pore waters

Jiajia Wang[1], Carolin F. Kerl[1], Pengjie Hu[2], Maria Martin[3], Tingting Mu[2], Lena Brüggenwirth[1], Guangmei Wu[2], Daniel Said-Pullicino[3], Marco Romani[4], Longhua Wu[2] and Britta Planer-Friedrich[1]*

[1]Environmental Geochemistry, Bayreuth Center for Ecology and Environmental Research (BayCEER), University of Bayreuth, 95440 Bayreuth, Germany.

[2]Key Laboratory of Soil Environment and Pollution Remediation, Institute of Soil Science, Chinese Academy of Sciences, 210008 Nanjing, China

[3]Department of Agriculture, Forest and Food Sciences, University of Turin, 10124 Turin, Italy

[4]Rice Research Centre, Ente Nazionale Risi, 27030 Castello d'Agogna, Pavia, Italy

*Phone: +49 921 55 3999. E-mail: b.planer-friedrich@uni-bayreuth.de.

Number of pages: 52

Number of figures: 20

Number of Tables: 9

1. Thioarsenates discovered in planted paddy fields in Italy and France

Methods. For an initial field survey, we sampled 23 different paddy fields in Italy (17 fields) and France (6 fields) (all located in the Mediterranean climate zone, for coordinates see Table S1) during the cropping season in August 2016 when the rice plants were in the flowering to grain filling stage. Sampling in Italy covered most of the rice cropping areas of the river Po plain, where the majority of the Italian rice is produced. The paddy fields were located in the alluvial plain, the river valley, and the lower river plain. All Italian soils developed on recent clastic deposits with mixed lithology (e.g., noncalcareous gravels, silty sands), and are mostly classified as luvisols, gleysols, and a few fluvisols and cambisols (Soil Atlas of Europe, https://esdac.jrc.ec.europa.eu/content/soil-atlas-europe). Paddy fields in France covered the whole extent of the only rice cultivation area in France which is located in the coastal plain of the Camargue region, in the delta of the river Rhone. The soils there developed on recent deposits of the Rhone river and are classified as gleyic fluvisols. In total, 35 pore-water samples were collected. At most paddy fields only one pore water sample was taken, at five paddy soils we took replicates. Pore-water was extracted by micro rhizon samplers (Rhizon MOM, Rhizosphere Research Products, The Netherlands) inserted about 3-4 cm deep into the paddy soil and connected to evacuated 100 mL glass bottles. The bottles were first sealed with a butyl rubber septum in an anoxic glovebox (N_2/H_2 95/5% (v/v)), then evacuated to negative atmospheric pressure of ~900 mbar. During sampling, glass bottles were shielded with aluminum foil to avoid potential photooxidation [1]. To retrieve enough volume (minimum 10 mL) for all analyses, minimum sampling time was 4 hours, maximum sampling time up to 24 hours. After retrieving the pore water samples, one soil sample from the plow layer was collected at each site.

After collection, pore-water samples were filtered through 0.2 µm cellulose-acetate filters. Samples for As speciation analysis were immediately flash-frozen on dry ice, and stored at -20 °C before being analyzed by ion chromatography (IC, Dionex ICS-3000) coupled to inductively coupled plasma-mass spectrometry (ICP-MS, XSeries2, Thermo-Fisher) at Bayreuth University following a previously established method for analysis of inorganic and methylated thioarsenates [2].

Retention times of the As species were verified by comparison with commercial standards (arsenite ($NaAsO_2$, Fluka), arsenate ($Na_2HAsO_4 \times 7H_2O$, Fluka), MMA ($CH_3AsNa_2O_3 \times 6H_2O$, Supelco), DMA ($C_2H_6AsNaO_2 \times 3H_2O$, Sigma-Aldrich)), standards synthesized according to previously published methods (DMMTA (purity 67%; 28% DMDTA, 5% DMA) and MMMTA (purity 96%; 1% MMA, 3% MMDTA) [3], MTA (purity of 98.5%; 0.5% arsenite, 1% arsenate)) [4] or by comparison with previously published [5] retention times (MMDTA, DMDTA, DTA, TTA). Calibration standard solutions were made from arsenate dibasic-heptahydrate, sodium (meta)arsenite, disodium methyl arsonate hexahydrate, and dimethylarsinic acid. All other As species were quantified by peak area comparison to the standard closest in retention time. Validity of this method has been proven previously [2].

An example of the chromatographic separation of the different As species is reported in Fig. S1. Samples for total As and Fe were acidified in 0.5% H_2O_2 and 0.8% HNO_3 and kept at 4°C until analysis by ICP-MS. Samples for zero-valent S were stabilized with zinc acetate (25 µL of 200 g/L ZnAc +725 µL sample), kept at 4°C until extraction by chloroform in the laboratory, then measured with high performance liquid chromatography (HPLC) (Merck Hitachi L-2130 pump, L-2200 autosampler, and L-2420 UV-VIS detector; C18 column, 100% methanol eluent at 0.2 mL/min) as described before [6]. Sulfide was measured photometrically on-site using the methylene blue method (HACH procedure No. 8131). Redox potential, pH, and conductivity were measured directly on-site by a WinLab redox micro-electrode, a WinLab 423 combination pH electrode, and a Mettler Toledo TetraCon 325 electrode.

Soil samples were analyzed for soil pH (measured in 2.5 mL 0.1 M $CaCl_2$ solution with 1 g soil), 0.5 M HCl-extractable Fe, total C and N (CHN analyzer), and total As and S (determination by ICP-MS after microwave digestion in aqua regia).

Results. Soil pH ranged from 5.0-6.1 and 7.5-7.6, total soil As contents from 5.2-16 and 10.4-20.2 mg/kg, HCl-extractable Soil Fe contents from 50-198 and 105-181 mmol/kg, and total C from 0.8-4.7 and 4.5-6.0 %, for the Italian and French paddy soils,

respectively (Table S1a). Thioarsenates were determined in 23 out of 35 pore-water samples and in 14 out of 23 different fields (Table S1b). The contribution of total thiolation to total As concentrations was 8.3% at maximum and 2.1% on average. These numbers are comparable to those observed for the much more-commonly-investigated methylated oxyarsenates which we detected in 31 samples from 20 fields (max. 10.4%, on average 1.3%). Inorganic thioarsenates (monothioarsenate (MTA) and dithioarsenate (DTA)) were detected in 11 samples (max. 7.4%, on average 3.2%) and methylated thioarsenates (monomethylmonothioarsenate (MMMTA), DMMTA, dimethyldithioarsenate (DMDTA)) in 18 samples (max. 2.9%, on average 0.7%). Seven samples taken within the same paddy field (Veronica, Table S1b) showed large heterogeneity in the proportion of thioarsenates (2.9-8.3%) without any obvious relation to pore-water chemistry, such as dissolved sulfide concentrations (Table S1b). Inorganic thioarsenates were observed in large quantities only at pore-water Fe concentrations < 0.5 mmol/L suggesting that Fe concentrations above a threshold value could limit their formation (Fig. S2a). Methylated thioarsenates, in contrast, occurred over a wider range of dissolved Fe concentrations (Fig. S2b) and Spearman´s correlation test showed positive correlation with methylated oxyarsenates ($r = 0.60$, $P<10^{-4}$; Fig. S2b, S2c, S3). There was no correlation between inorganic and methylated thioarsenates.

For these first field surveys, we used relatively long pore-water sampling times (4-24 hours) to obtain enough volume for analyses (minimum 10 mL) and, for species preservation, we used just flash-freezing, without adding stabilizing agents. Even though all As chromatographic peaks were clearly distinguishable (Fig. S1), high Fe concentrations (up to 2.3 mmol/L) caused Fe precipitation and, by co-precipitation and sorption, low As recoveries (calculated as the sum of all detected As species in flash-frozen samples versus total As measured in oxidized and acid-stabilized samples; Fig. S4).

All species proportions are reported with respect to total As (not the sum of species). As such, a partial precipitation or sorption of thiolated As species on any Fe (hydr)oxides [7] formed during sample storage could have contributed to an underestimation of the true proportions reported here.

For all later analyses, short sampling times (0.5-1 hour) and an optimized DTPA-sample stabilization and analysis were chosen. For details on the DTPA method development and evaluation see main manuscript and Fig. S15-S18.

Table S1a | Coordinates and basic soil chemistry from 17 Italian paddy fields (IT) and 6 French paddy fields (FR)

Paddy fields	Longitude	Latitude	Soil pH	HCl extract-able soil Fe	total soil As	total soil S	total soil C
				mmol/kg	mg/kg	g/kg	%
ITALY							
IT_Vignarello	8°44′42.82″	45°20′39.77″	5.5	62.6	8.9	3.4	2.0
IT_Barbavara	8°47′09.49″	45°21′19.41″	5.5	67.6	10.5	3.2	2.7
IT_Gambarana	8°46′30.88″	45°01′38.88″	5.8	197.7	16.0	6.0	1.4
IT_Breme	8°37′06.19″	45°08′38.34″	5.8	177.0	13.8	5.4	1.3
IT_Langosco	8°32′43.84″	45°12′34.24″	5.7	165.5	12.9	8.4	1.3
IT_Vercelli	8°15′12.88″	45°18′36.59″	5.7	75.9	11.4	9.5	1.1
IT_Cascina Oschiena	8°45′03.84″	45°18′36.58″	5.7	109.9	6.1	4.2	1.3
IT_Fontanetto Po	8°11′59.46″	45°12′15.50″	6.0	144.9	9.1	4.8	3.4
IT_Terranova	8°30′02.95″	45°11′53.56″	6.1	125.3	11.8	5.3	1.4
IT_Rovasenda	8°16′40.00″	45°32′34.05″	5.8	97.2	14.3	4.3	1.0
IT_Cascina Albera	8°56′48.18″	45°10′49.49″	5.8	52.0	5.9	2.7	1.4
IT_Lomello	8°47′55.87″	45°07′26.71″	5.0	120.6	8.9	4.1	1.4
			5.6	90.2	7.3	3.9	1.5
IT_Cascina Fornazzo	8°57′49.97″	45°13′53.76″	5.8	71.7	5.6	3.2	4.7
IT_Cascina Veronica	8°53′47.60″	45°10′39.30″	5.6	50.0	5.2	2.2	2.1
			5.5	53.0	5.8	2.6	2.0
			5.4	50.6	5.8	2.4	1.9
IT_Castello d´Agogna (ENR) field 1	8°41′56.50″	45°14′51.30″	5.5	145.9	16.0	4.3	0.9
			5.5	152.3	15.6	4.3	0.8
IT_Castello d´Agogna (ENR) field 2			5.5	146.7	15.2	4.4	0.8
			5.5	144.1	15.6	4.2	0.8

IT_Castello d´Agogna (ENR) field 3			5.6	181.0	15.8	4.2	0.9
			5.5	159.3	14.9	4.2	0.9
FRANCE							
FR_Seyne	4°42′57.24″	43°34′23.63″	7.5	166.0	18.2	22.1	5.4
FR_Vedeau	4°42′24.53″	43°26′04.63″	7.6	143.0	14.7	23.1	6.0
FR_Adrien	4°33'40.93''	43°42'07.42''	7.5	109.5	10.4	18.0	4.9
FR_Furane	4°31′06.35″	43°41′11.58″	7.5	134.1	20.2	19.8	4.9
FR_Boismeaux	4°28′14.10″	43°35′54.44″	7.5	138.9	13.1	18.8	4.5
FR_Signore	4°29′46.35″	43°37′10.51″	7.6	104.7	10.6	22.6	5.2

Table S1b | Pore water chemistry including As speciation for samples from 17 Italian paddy fields (IT) and 6 French paddy fields (FR)

Paddy fields	pore water pH	E_H	Conductivity	Sulfide	Zerovalent sulfur	Fe	DMA	DMMTAa	Arsenite	DMDTA[b]	MMA	MMTA[c]	Arsenate	MTA[d]	DTA[e]	Total Thiolated As	Sum As species	Total As
		mV	µS/cm	µmol/L		mmol/L	µg/L											
ITALY																		
IT_Vignarello	6.1	194	310	<0.3	4.6	0.3	0.2		2.8				1.0				3.9	38.1
IT_Barbavara	6.6	184	305	<0.3	2.4	0.2	0.04		0.5				0.2				0.7	10.6
IT_Gambarana	6.9	71	1154	<0.3	<1	0.3	0.1		3.1		0.3		2.5				6.1	86.2
IT_Breme	6.6	-21	1340	<0.3	4.3	2.6	0.4		1.1		0.4	0.2	0.3			0.2	2.4	82.0
IT_Langosco	6.4	145	575	<0.3	5.4	0.9	0.2	0.2	0.5		0.1	0.1	0.2			0.3	1.3	37.3
IT_Vercelli	6.3	339	209	<0.3	<1	0.0			1.9				1.6				3.4	7.8
IT_Cascina Oschiena	6.5	72	1092	1.2	<1	1.5		0.1	0.5				0.2			0.1	0.9	68.2
IT_Fontanetto Po	7.0	377	1831	1.2	<1	<0.1	0.1		2.7		0.1		1.0				3.9	9.0
IT_Terranova	7.0	68	2490	1.3	5.8	0.2	1.5	0.1	11.8				2.3			0.1	15.8	84.2
IT_Rovasenda	6.6	116	370	1.2	<1	0.1	0.6	0.1	0.3				0.4			0.1	1.4	6.0

IT_Cascina Albera	6.7	93	315	1.8	1.2	0.6	0.1		1.4			0.04	0.3			0.04	1.8	31.3
IT_Lomello	6.8	92	280	0.9	2.7	0.1			1.4				0.4				1.8	25.9
	7.0	97	362	<0.3	5.2	0.0	0.2		2.6		0.1		2.3	0.2		0.2	5.5	15.2
IT_Cascina Fornazzo	7.1	98	673	<0.3	5.2	0.3	0.5	0.1	1.3		0.2	0.3	0.5	0.1	0.2	0.8	3.3	14.9
IT_Cascina Veronica	6.4	90	541	<0.3	<1	0.5	0.6	0.4	1.8	0.1	0.1	0.03	0.6	0.2	0.4	1.2	4.4	28.2
	6.2	122	341	<0.3	<1	0.3		0.1	0.9			0.1	0.7	0.2	0.2	0.5	2.1	9.1
	6.4	83	n.a	3.0	<1	0.3			1.6		0.04	0.0	3.8	0.4	0.3	0.8	6.2	17.7
Paddy fields	**pore water pH**	**E_H**	**Conductivity**	**Sulfide**	**Zerovalent sulfur**	**Fe**	**DMA**	**DMMTAa**	**Arsenite**	**DMDTA[b]**	**MMA**	**MMMTA[c]**	**Arsenate**	**MTA[d]**	**DTA[e]**	**Total Thiolated As**	**Sum As species**	**Total As**
		mV	**µS/cm**	**µmol/L**		**mmol/L**	**µg/L**											
IT_Cascina Veronica	6.3	117	285	1.1	<1	0.3			2.8		0.2	0.1	1.8	0.3	0.6	1.0	5.8	11.9
	n.a.	n.a.	n.a.	<0.3	<1	0.3			2.3		0.1		6.9	0.5	0.2	0.8	10.1	20.6
	6.5	169	n.a.	<0.3	1.8	0.3			0.7		0.05		1.2	0.2	0.3	0.5	2.4	8.0

	6.2	105	400	<0.3	<1	0.3	0.03		0.4		0.1		0.7	0.1	0.1	0.2	1.5	7.1
IT_Castello d´Agogna (ENR) field 1	6.8	-13	1183	1.0	1.5	1.8	0.1	0.3	0.6		0.5		0.1			0.3	1.6	105.4
	6.6	85	723	<0.3	<1	0.8	0.1		0.6				0.3				1.0	44.4
IT_Castello d´Agogna (ENR) field 2	6.7	83	n.a.	1.1	2.4	0.6	0.1	0.03	0.7				0.2			0.03	1.0	30.0
	6.8	1	1346	1.0	<1	1.8	0.1	0.1	0.5		0.3	0.1	0.1			0.2	1.2	58.5
	6.8	44	1181	<0.3	<1	0.8	0.2	0.1	0.5		0.5	0.2	0.1			0.3	1.6	24.8
	6.7	70	890	<0.3	<1	1.2	0.1	0.1	0.4		0.2		0.1			0.1	0.9	36.7
IT_Castello d´Agogna (ENR) field 3	6.7	83	792	<0.3	3.8	0.7	0.1		1.2		0.1		0.2				1.6	45.4
	6.8	117	364	<0.3	2.8	0.3	0.1		2.0				0.6				2.6	47.1
FRANCE																		
FR_Seyne	7.2	37	1030	<0.3		0.5			1.9				0.2				2.1	72.8
FR_Vedeau	6.8	32	2200	<0.3		0.7	1.4		6.7				0.5				8.6	165.2
FR_Adrien	7.3	91	1340	<0.3		0.2	0.2	0.1	21.9		0.04		2.8	0.2	0.1	0.4	25.3	86.7
FR_Furane	7.2	-16	1854	<0.3		1.4	1.0	0.1	11.				2.5			0.1	15.	335.

									7								3	2
FR_Boismeaux	7.3	16	2010	<0.3		1.2	1.1	0.4	16.8	0.1	0.9	0.2	2.5	0.1		0.8	22.2	268.3
FR_Signore	7.5	37	1509	<0.3		0.6	0.3		4.4		0.1		0.4				5.3	69.5

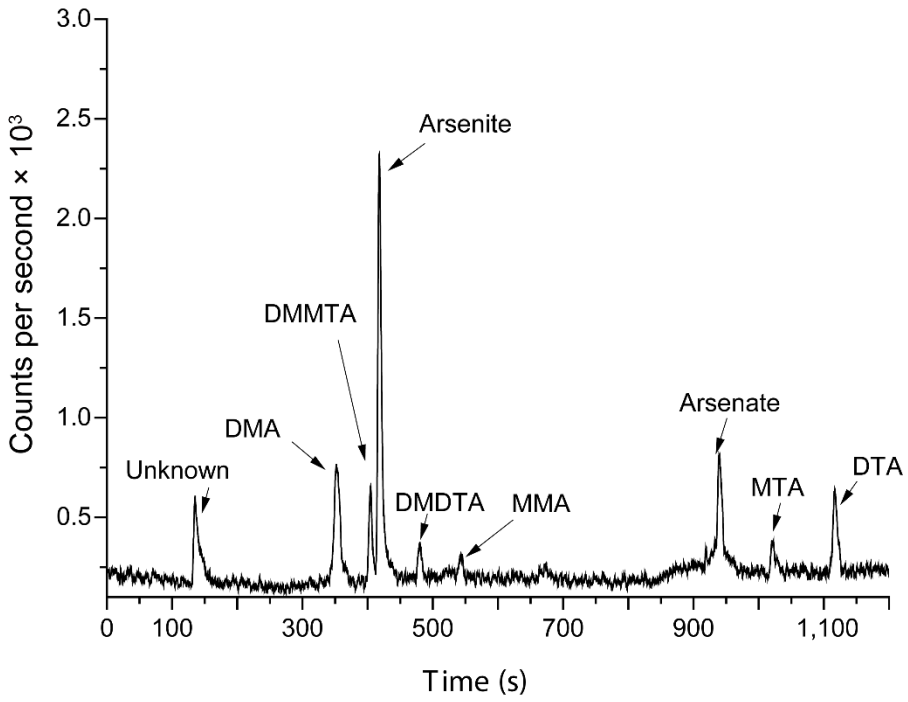

Figure S1 | Example chromatogram for determination of inorganic and methylated thio and oxy As species in paddy field pore-water by IC-ICP-MS. The presented sample is IT_Cascina Veronica (pH 6.36, Table S1).

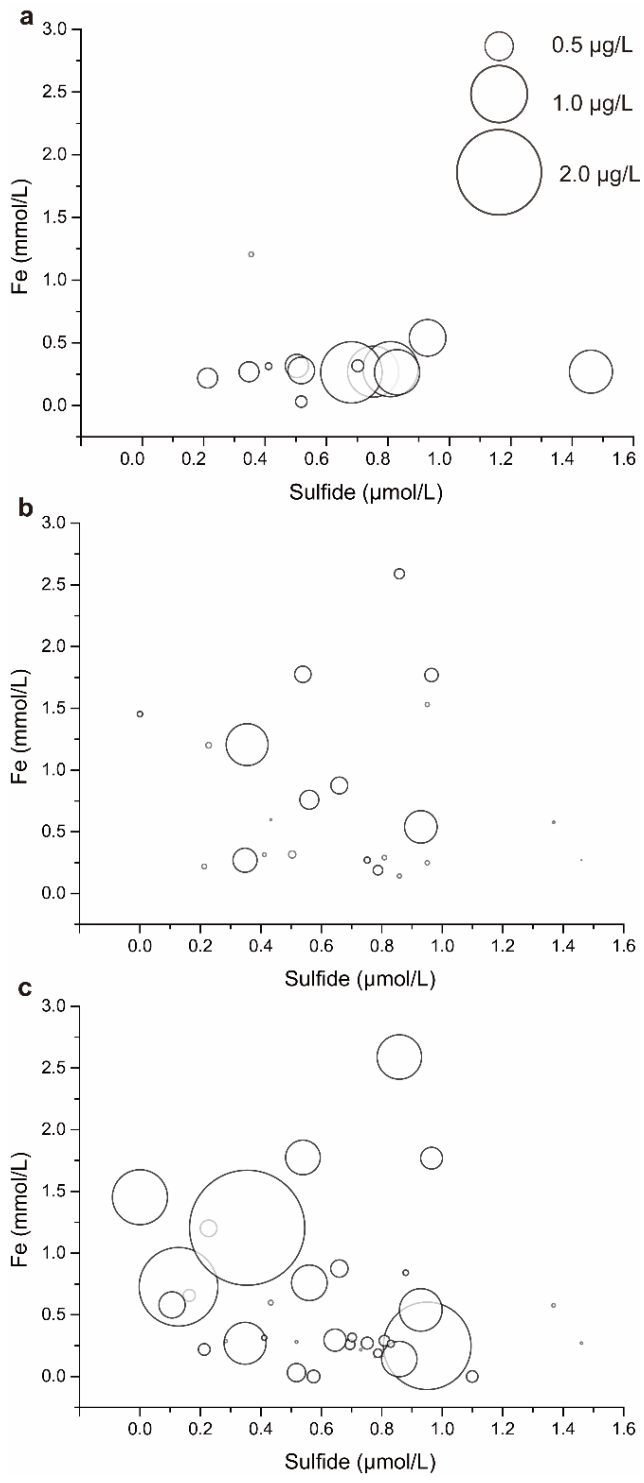

Figure S2 | Arsenic speciation in paddy field pore-waters from Italy and France in relation to aqueous Fe and sulfide. Contribution of a) inorganic thioarsenates, b) methylated thioarsenates and c) methylated oxyarsenates to total As; bubble size

represents concentration of As species; bubbles are only displayed where concentrations of As species were above detection limit.

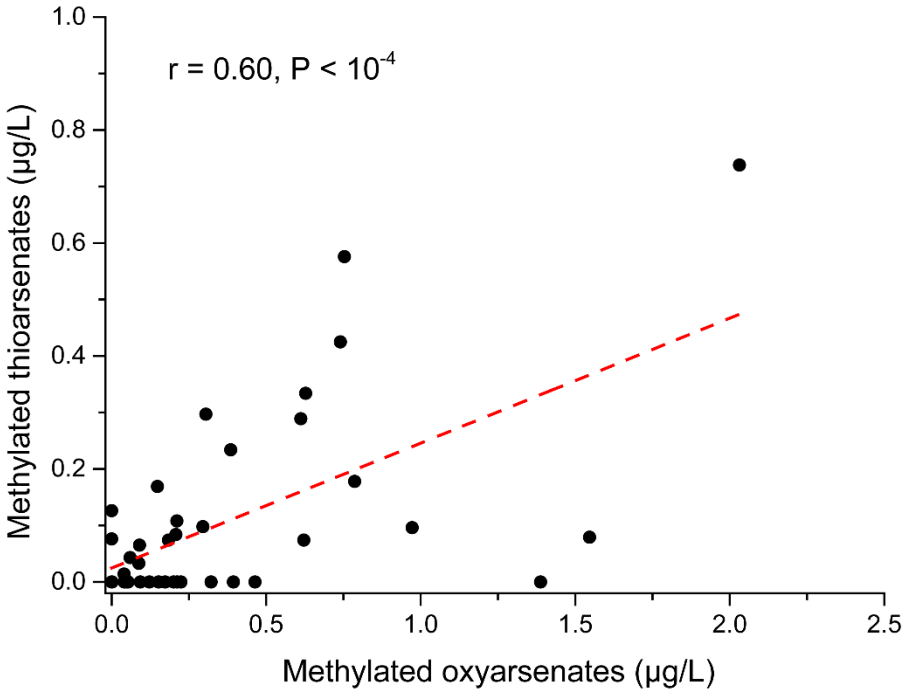

Figure S3 | Correlation of methylated thioarsenates with methylated oxyarsenates in paddy field pore-waters from Italy and France.

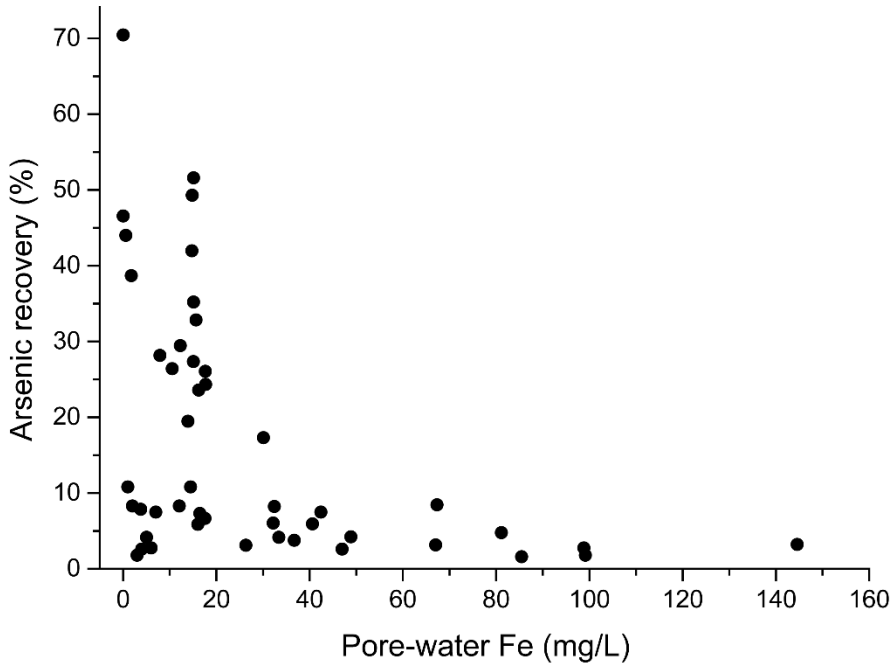

Figure S4 | Effect of Fe on As recovery for samples from paddy fields in Italy and France. Arsenic recovery is calculated as sum of As species from flash-frozen samples versus total As in H_2O_2-HNO_3-stabilized samples.

2. Mesocosm rice cultivation experiments – effects of sulfate-fertilization, seeding-practice, and soil type on thioarsenate formation

Looking at the pore-water total As concentrations during rice cultivation in the mesocosm experiments (Fig 2), one can see that over time, pore-water total As concentrations in control treatments decreased from approximately 100 and 50 µg/L at tillering stage in the dry and water seeded mesocosms, respectively, to <20 µg/L around flowering stage (except for the dry seeded Veronica soil where concentrations only dropped after the dough stage, Fig. 2e, f). Highest pore-water As concentrations occurred within days after flooding due to rapid As mobilization by reductive dissolution of Fe(III)-(oxy)hydroxides, and then decreased due to As re-adsorption on or precipitation with newly formed Fe minerals in line with previous reports [8, 9]. The higher As concentrations in dry vs. water seeded treatments at the same sampling date could be explained by an overall less As mobilization in water seeded treatments because they are flooded in May when microbially catalyzed As mobilization is still partially limited by lower temperatures while flooding of dry seeded treatments in June leads to higher As mobilization due to enhanced microbial activity. In addition, the difference could reflect the time it takes for As concentrations after flooding and initial mobilization to drop again due to re-adsorption and precipitation reactions (4 weeks later in dry than in water seeded treatments). No clear trend in the proportion of inorganic or methylated thioarsenates was observed over time (Fig. 2a-d).

Table S2 | Soil classification and basic chemical parameters for Veronica and Fornazzo soil

Parameters	**Veronica**	**Fornazzo**
Geology/geomorphology	Lower river plain	Valley of the Ticino river
Parent material	Pleistocene alluvium	Olocene alluvium
Soil classification		
USDA	Aeric Endoacquepts coarse-loamy over sandy, mixed, mesic	Histic Humaquepts coarse-loamy, mixed, mesic
FAO	Eutric Gleysoil	Umbric Gleysoil
Texture		
gravel (%weight)	nd	23.9
clay %	2.1	1.4
fine silt %	11.5	6.2
coarse silt %	8.8	6.8
fine sand %	18.2	23.7
coarse sand %	59.3	61.8
Cation exchange capacity (cmol /kg)	9.52	14.39
Base saturation (%)	0.24	0.24
Effective base saturation (%)	0.84	0.91
soil pH	5.6	5.8
0.5 M HCl-extractable Fe (mmol/kg)	52	71
Oxalate-extracted Fe (mmol/kg)	9.9	19.2
C (%)	2.0	4.7
N (%)	0.6	0.5
Total As (mg/kg)	5.8	5.6

Oxalate-extracted As (mg/kg)	1.4	1.5
S (g/kg)	2.6	3.2

Table S3 | Pore water chemistry at different rice growing stages in the mesocosm experiments (2017) separated by soil type, fertilization (non-sulfate/sulfate), and seeding practice (dry-seeding/wet-seeding) (n=3)

Pore water parameters	Soil type & Seeding practice	Fertili-zation	Jun 14th	Jul 4th	Jul 18th	Aug 1st	Aug 8th	Aug 22th	Sep 13th
			Tillering	Stem elongation	Booting	Flowering	Grain filling	Dough	Mature
pH	**Veronica**								
	water-seeding	non-sulfate	6.9 ± 0.1	6.8 ± 0.1	6.7 ± 0.2	6.5 ± 0.1	6.5 ± 0.1	6.8 ± 0.1	6.8 ± 0.1
		sulfate	6.9 ± 0.1	6.9 ± 0.2	6.6 ± 0.1	6.8 ± 0.1	6.7 ± 0.1	7.1 ± 0.1	6.8 ± 0.2
	dry-seeding	non-sulfate	6.8 ± 0.3	6.5 ± 0.4	6.5 ± 0.1	6.4 ± 0.1	6.5 ± 0.1	6.8 ± 0.3	6.6 ± 0.1
		sulfate	6.8 ± 0.2	6.9 ± 0.1	6.7 ± 0.1	6.7 ± 0.1	6.8 ± 0.2	7.0 ± 0.1	6.8 ± 0.1
	Fornazzo								
	water-seeding	non-sulfate	7.2 ± 0.2	7.3 ± 0.1	7.2 ± 0.1	7.1 ± 0.1	7.2 ± 0.1	7.2 ± 0.2	7.3 ± 0.2
		sulfate	7.0 ± 0.1	7.1 ± 0.1	6.9 ± 0.1	7.1 ± 0.1	7.1 ± 0.1	7.5 ± 0.1	7.1 ± 0.1
	dry-seeding	non-sulfate	7.0 ± 0.1	7.0 ± 0.3	7.2 ± 0.1	7.0 ± 0.1	7.1 ± 0.1	7.2 ± 0.1	7.4 ± 0.1
		sulfate	7.2 ± 0.1	7.2 ± 0.2	7.3 ± 0.1	7.0 ± 0.04	7.1 ± 0.1	7.3 ± 0.1	7.4 ± 0.1

E_H (mV)	**Veronica**								
	water-seeding	non-sulfate	181 ± 85	168 ± 62	185 ± 56	122 ± 5	161 ± 9	179 ± 19	160 ± 26
		sulfate	123 ± 25	131 ± 36	159 ± 24	92 ± 16	121 ± 11	149 ± 18	126 ± 16
	dry-seeding	non-sulfate	212 ± 44	163 ± 9	162 ± 11	180 ± 98	163 ± 5	165 ± 11	167 ± 24
		sulfate	207 ± 59	135 ± 30	127 ± 47	89 ± 30	130 ± 17	131 ± 31	129 ± 16
	Fornazzo								
	water-seeding	non-sulfate	181 ± 81	163 ± 15	148 ± 59	116 ± 19	103 ± 19	130 ± 36	118 ± 26
		sulfate	96 ± 2	112 ± 50	87 ± 7	69 ± 10	77 ± 20	80 ± 11	84 ± 13
	dry-seeding	non-sulfate	287 ± 6	211 ± 4	132 ± 43	111 ± 37	126 ± 11	135 ± 5	130 ± 29
		sulfate	163 ± 61	143 ± 37	193 ± 75	109 ± 75	119 ± 35	146 ± 20	143 ± 51
Conductivity (µS/cm)	**Veronica**								
	water-seeding	non-sulfate	533 ± 92	325 ± 30	504 ± 83	580 ± 54	777 ± 13	667 ± 263	601 ± 170
		sulfate	745 ± 374	382 ± 165	455 ± 51	412 ± 34	493 ± 111	386 ± 59	567 ± 21

	dry-seeding	non-sulfate	805 ± 184	324 ± 41	554 ± 153	630 ± 52	835 ± 89	693 ± 38	651 ± 76
		sulfate	614 ± 52	335 ± 72	434 ± 59	631 ± 424	414 ± 64	345 ± 37	478 ± 66
	Fornazzo								
	water-seeding	non-sulfate	956 ± 54	932 ± 94	1128 ± 95	1171 ± 118	1362 ± 120	1392 ± 211	1469 ± 223
		sulfate	1026 ± 116	781 ± 32	922 ± 60	1038 ± 208	955 ± 64	1051 ± 147	1188 ± 10
	dry-seeding	non-sulfate	723 ± 113	909 ± 63	1102 ± 24	1133 ± 49	1281 ± 37	1397 ± 125	1416 ± 130
		sulfate	988 ± 124	846 ± 79	1483 ± 731	876 ± 119	841 ± 65	866 ± 69	1016 ± 102
TIC (mg/L)[a]	**Veronica**								
	water-seeding	non-sulfate	14.16 ± 2.79	19.46 ± 1.75	15.65 ± 0.96	16.7 ± 2.62	10.42 ± 1.14	15.81 ± 5.37	20.44 ± 6.69
		sulfate	15.78 ± 4.27	15.41 ± 4.62	20.33 ± 7.46	25.44 ± 5.94	33.57 ± 10.36	28.73 ± 3.37	31.52 ± 3.61
	dry-seeding	non-sulfate	21.86 ± 8.47	18.01 ± 0.8	14.13 ± 0.9	12.77 ± 1.39	13.28 ± 9.72	10.48 ± 1.57	15.12 ± 0.65
		sulfate	19.2 ± 1.69	22.34 ± 7.27	23.76 ± 6.24	25.16 ± 5.07	23.51 ± 5.28	24.81 ± 3.58	25.67 ± 3.73
	Fornazzo								

	water-seeding	non-sulfate	43.14 ± 12.93	88.92 ± 7.44	90.41 ± 8.63	100.94 ± 12.11	82.72 ± 7.89	96.99 ± 17.99	108.12 ± 22.39
		sulfate	50.36 ± 10.5	76.07 ± 3.13	77.13 ± 0.79	89.25 ± 0.76	84.85 ± 9.04	99.84 ± 5.25	107.10 ± 5.75
	dry-seeding	non-sulfate	66.67 ± 24.6	79.01 ± 6.86	75.84 ± 6.10	81.57 ± 12.66	61.97 ± 38.60	77.89 ± 1.59	85.61 ± 1.77
		sulfate	86.25 ± 10.75	85.05 ± 9.16	79.54 ± 6.38	83.88 ± 6.11	98.32 ± 14.63	85.61 ± 6.21	89.12 ± 7.56
TOC (mg/L)[b]	**Veronica**								
	water-seeding	non-sulfate	23.03 ± 2.46	94.27 ± 25.89	101.71 ± 63.16	91.58 ± 60.92	73.44 ± 50.96	64.89 ± 41.32	59.91 ± 32.46
		sulfate	30.63 ± 5.57	85.81 ± 32.97	93.45 ± 44.74	95.54 ± 47.79	91.58 ± 50.61	94.95 ± 53.44	92.03 ± 49.37
	dry-seeding	non-sulfate	59.09 ± 21.00	58.73 ± 3.22	64.16 ± 6.93	61.25 ± 1.29	49.09 ± 5.30	46.03 ± 3.51	47.33 ± 3.09
		sulfate	47.92 ± 6.44	57.30 ± 6.04	57.80 ± 6.06	57.92 ± 15.69	65.77 ± 12.15	57.25 ± 25.19	51.22 ± 25.59
	Fornazzo								
	water-seeding	non-sulfate	73.85 ± 44.24	135.92 ± 21.00	147.04 ± 48.47	131.41 ± 49.74	102.8 ± 24.21	96.37 ± 35.54	94.20 ± 34.24
		sulfate	56.46 ± 11.03	116.33 ± 26.03	110.91 ± 21.76	105.03 ± 10.82	95.76 ± 3.61	104.26 ± 10.07	99.93 ± 18.22

	dry-seeding	non-sulfate	96.47 ± 17.48	105.86 ± 6.54	121.54 ± 9.10	118.47 ± 17.25	103.63 ± 7.21	80.97 ± 5.29	81.18 ± 10.63
		sulfate	96.73 ± 10.32	108.26 ± 2.00	113.3 ± 20.63	109.97 ± 28.59	138.61 ± 38.75	106.29 ± 36.38	107.84 ± 42.60
Fe^{II}(mmol/L)[c]	**Veronica**								
	water-seeding	non-sulfate	0.23 ± 0.02	0.25 ± 0.01	0.29 ± 0.04	0.31 ± 0.07	0.45 ± 0.03	0.34 ± 0.14	0.28 ± 0.07
		sulfate	0.22 ± 0.03	0.27 ± 0.02	0.25 ± 0.06	0.28 ± 0.07	0.34 ± 0.06	0.29 ± 0.07	0.25 ± 0.06
	dry-seeding	non-sulfate	0.07 ± 0.04	0.20 ± 0.01	0.29 ± 0.03	0.35 ± 0.03	0.48 ± 0.04	0.43 ± 0.01	0.33 ± 0.00
		sulfate	0.08 ± 0.02	0.25 ± 0.02	0.26 ± 0.01	0.26 ± 0.04	0.31 ± 0.04	0.30 ± 0.04	0.24 ± 0.04
	Fornazzo								
	water-seeding	non-sulfate	0.32 ± 0.07	0.43 ± 0.04	0.43 ± 0.03	0.43 ± 0.04	0.48 ± 0.03	0.41 ± 0.06	0.40 ± 0.03
		sulfate	0.34 ± 0.05	0.40 ± 0.08	0.36 ± 0.05	0.37 ± 0.06	0.40 ± 0.03	0.39 ± 0.03	0.35 ± 0.04
	dry-seeding	non-sulfate	0.11 ± 0.04	0.34 ± 0.01	0.40 ± 0.01	0.42 ± 0.04	0.49 ± 0.04	0.47 ± 0.03	0.42 ± 0.04
		sulfate	0.14 ± 0.09	0.37 ± 0.05	0.37 ± 0.04	0.37 ± 0.07	0.44 ± 0.08	0.40 ± 0.08	0.37 ± 0.05

Total As (µg/L)	**Veronica**								
	water-seeding	non-sulfate	48.18 ± 19.47	41.19 ± 10.28	31.62 ± 10.10	17.81 ± 4.89	12.12 ± 2.74	7.67 ± 1.55	5.57 ± 1.30
		sulfate	24.24 ± 11.77	11.19 ± 1.07	9.26 ± 1.73	10.20 ± 2.27	11.71 ± 2.98	9.69 ± 4.03	7.58 ± 2.62
	dry-seeding	non-sulfate	104.09 ± 9.14	83.34 ± 17.86	76.40 ± 11.97	46.93 ± 13.39	31.76 ± 8.53	18.40 ± 5.70	7.57 ± 1.73
		sulfate	72.61 ± 15.21	8.04 ± 0.84	6.97 ± 0.86	7.69 ± 1.05	10.04 ± 1.10	8.71 ± 1.27	5.41 ± 1.25
	Fornazzo								
	water-seeding	non-sulfate	48.02 ± 4.66	22.02 ± 2.44	19.80 ± 3.80	19.65 ± 4.60	18.58 ± 4.58	15.63 ± 3.34	13.30 ± 3.22
		sulfate	27.64 ± 4.80	18.45 ± 1.07	16.04 ± 1.38	15.51 ± 0.75	15.21 ± 0.55	14.05 ± 0.41	12.19 ± 0.74
	dry-seeding	non-sulfate	97.32 ± 7.49	61.53 ± 13.53	25.32 ± 2.57	20.85 ± 0.66	19.72 ± 1.27	17.00 ± 1.62	14.91 ± 1.82
		sulfate	76.46 ± 9.82	23.37 ± 1.56	19.29 ± 1.46	17.89 ± 2.19	16.99 ± 2.51	14.65 ± 2.69	12.71 ± 2.78

[a] Total inorganic carbon; [b] Total organic carbon;[c] Fe^{II} was spectrophotometricaly determinated via 1,10-phenanthroline method.

Table S4 | Mean values for thiolation and methylation (integrated over the seven sampling times) for comparison of factors of increases by sulfate-addition (ratio S/no S) for the two different soil types (Veronica/Fornazzo) and water- vs. dry-seeding

	water-seeding			**dry-seeding**	
Inorganic thioarsenates	Veronica	Fornazzo		Veronica	Fornazzo
contribution to As speciation - no S [%]	3.0	1.8		0.6	1.3
contribution to As speciation - S [%]	4.7	5.5		3.9	2.6
ratio S/noS	1.5	3.1		6.4	2.1
Methylated thioarsenates	Veronica	Fornazzo		Veronica	Fornazzo
contribution to As speciation - no S [%]	0.1	0.9		0.2	1.0
contribution to As speciation - S [%]	2.1	1.4		1.7	1.7
ratio S/noS	19.8	1.6		11.6	1.8
Total Thiolation	Veronica	Fornazzo		Veronica	Fornazzo
contribution to As speciation - no S [%]	3.1	2.7		0.8	2.2
contribution to As speciation - S [%]	6.8	6.9		5.6	4.3

ratio S/noS	2.2	2.5		7.4	2
Methylated oxyarsenates	Veronica	Fornazzo		Veronica	Fornazzo
contribution to As speciation - no S [%]	5.0	5.6		2.1	4.4
contribution to As speciation - S [%]	12.7	5.2		11.1	6.1
ratio S/noS	2.6	0.9		5.3	1.4

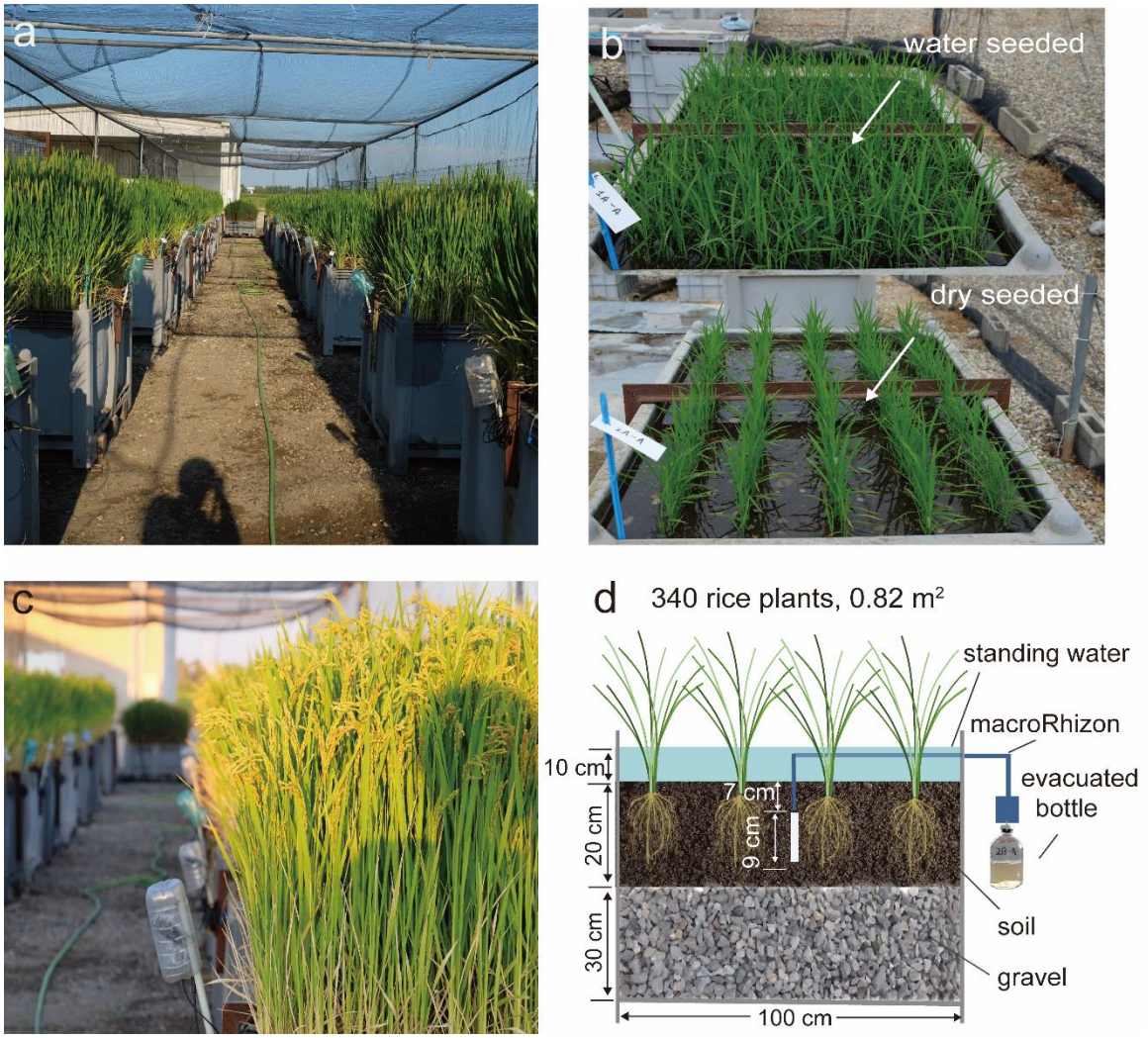

Figure S5 | Photos and schematic design of the mesocosm rice cultivation experiments. A total of 24 mesocosms with 2 different soil types, water and dry seeded, with and without sulfate fertilization (each setup conducted in triplicates) were installed at the Rice Research Centre Ente Nazionale Risi in Castello d'Agogna (Pavia, Italy); a) flowering stage; b) seeding practices; c) mature stage; d) scheme of the setup.

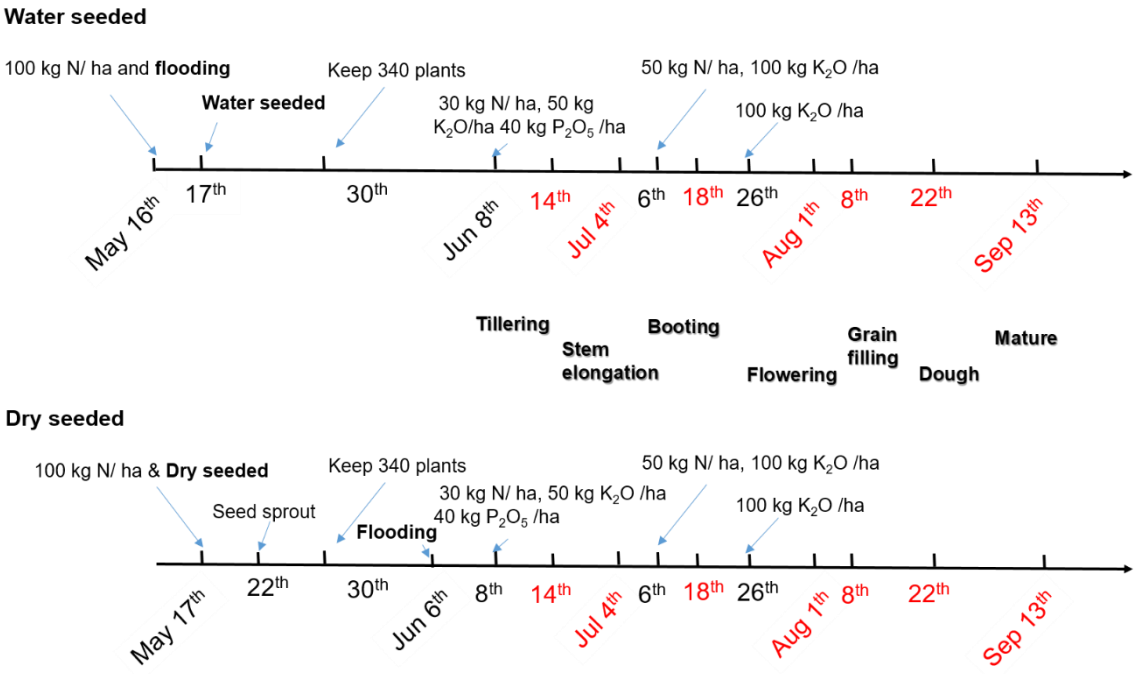

Figure S6 | Agronomic management of water and dry seeded mesocosm rice cultivation experiments in 2017. For sulfate treatments, ammonium sulfate and potassium sulfate were applied, while urea and potassium chloride were used equivalent in N and K for control treatments. Dates in red indicate pore-water sampling dates.

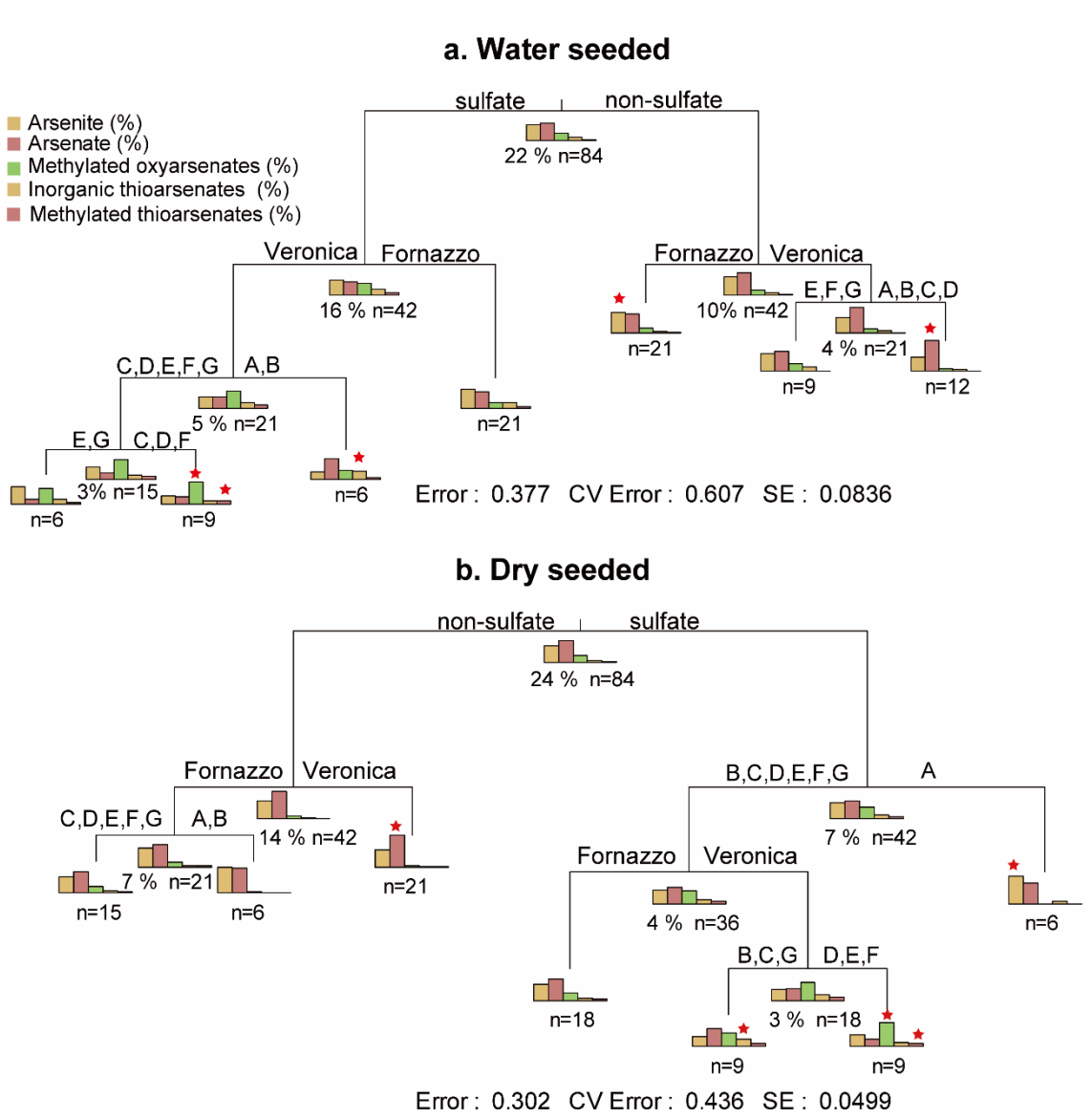

Figure S7 | Multivariate regression tree for pore-water As speciation in the mesocosm experiments for a) water seeded and b) dry seeded treatments. Multivariate regression tree analyses were done following previously published methods[10]. Capital letters A-G on the node represent the seven rice growth stages from tillering stage to maturity. Indicator species, based on relative abundance and relative frequency of occurrence of As species, are denoted by stars. Pre-separation in water and dry seeded was done because different redox regimes lead to an offset of growth stages in dry seeded compared to water seeded treatments by about 7-10 days.

3. Incubation experiments revealing soil properties that determine the potential for thioarsenate formation

Table S5a | Location, parent material, and soil classification of 31 paddy soils sampled in China.

No.	Location	Longitude	Latitude	Parent material	Soil classification (within the suborder Stagnic Anthrosols[a])
CH1	Jiangmen, Guangdong	112º31′09.2″	22º30′33.9″	river alluvium	Fe-accumuli-
CH2	Nanning 2, Guangxi	108º17′12.6″	23º06′22.4″	limestone	Fe-accumuli-
CH3	Nanning1, Guangxi	108º16′52.0″	23º06′27.6″	limestone	Fe-accumuli-
CH4	Dehong, Yunnan	98º25′55.1″	24º26′31.11″	river alluvium	Fe-accumuli-
CH5	Chuxiong, Yunnan	102º03′5.71″	25º11′01.3″	river alluvium (sandy)	Fe-leachi-
CH6	Ganzhou, Jiangxi	114º27′11.8″	25º26′31.8″	river alluvium	Fe-accumuli-
CH7	Guiyang, Guizhou	106º40′17.6″	26º20′12.7″	limestone	Fe-leachi-
CH8	Qiandongnan, Guizhou	108º03′43.19″	26º36′46.71″	limestone	Fe-leachi-
CH9	Sanming, Fujian	117º10′30.44″	26º50′56.14″	river alluvium	Fe-accumuli-
CH10	Ji'an, Jiangxi	114º54′36.0″	26º58′21.4″	river alluvium	Fe-accumuli-
CH11	Zunyi, Guizhou	106º48′14.5″	27º30′13.15″	limestone	Hapli-

CH12	Yingtan, Jiangxi	117º15′21.1″	28º20′31.1″	river alluvium	Fe-accumuli-
CH13	Yueyang, Hunan	113°5'43.8''	29°14'23.0''	lacustrine deposits	Fe-accumuli-
CH14	Jinhua, Zhejiang	119º20′34.1″	29º01′04.9″	river alluvium	Hapli-
CH15	Jingzhou, Hubei	112º 31′49.03″	30º 5′53.10″	river alluvium	Fe-accumuli-
CH16	Hangzhou, Zhejiang	120º05′13.3″	30º28′05.6″	river alluvium	Fe-accumuli-
CH17	Jiaxing, Zhejiang	121º07′01.26″	30º48′06.3″	marine sediment	Fe-leachi-
CH18	Zhenjiang, Jiangsu	119º18′15.47″	31º57′58.38″	river alluvium	Fe-leachi-
CH19	Xuancheng,Anhui	118º29′55.7″	31º00′02.6″	river alluvium	Hapli-
CH20	Hefei, Anhui	117º13′28.1″	31º35′54.1″	lacustrine deposits	Fe-accumuli-
CH21	Xinyang, Henan	114º59′03″	31º54′13″	river alluvium (loess)	Fe-accumuli-
CH22	Hanzhong, Shaanxi	106º54′36.15″	33º09′37.77″	loess	Fe-leachi-
CH23	Yancheng, Jingsu	120º04′10.6″	33º16′12.5″	marine sediment	Fe-accumuli-
CH24	Xuzhou, Jiangsu	117º24′38.49″	34º17′46.59″	river alluvium	Fe-leachi-
CH25	Lianyungang, Jiangsu	119º20′06.1″	34º32′58.0″	river alluvium	Fe-leachi-
CH26	Jining, Shandong	116º33′32.5″	35º18′47.7″	river alluvium	Fe-accumuli-
CH27	Yinchuan, Ningxia	106º16′0.97″	38º10′04.78″	river alluvium	Hapli-
CH28	Panjin, Liaoning	122º13′46.6″	40º58′26.09″	marine sediment	Hapli-
CH29	Siping, Jilin	124º42′29.1″	43º28′47.8″	river alluvium	Hapli-
CH30	Wuchang, Heilongjiang	127º02′12.9″	45º03′42.1″	river alluvium	Hapli-

CH31	Jiamusi, Heilongjiang	131°36′34.2″	47°11′12.8″	river alluvium	Hapli-

[a] Based on the Chinese Soil Taxonomic Classification (adopted by WRB in 1998) all paddy soils used here are classified as Stagnic Anthrosols. Stagnic Anthrosols are anthrosols that have an anthrostagnic moisture regime, and both a hydragric epipedon (including a cultivated horizon and a plowpan) and a hydragric horizon.

Table S5b | Geology/geomorphology and climate zones of the 31 paddy fields sampled in China.

No.	Geology/Geomorphology	Climate Zone
CH1	The lower hilly and wide valley basin of Jiangmen	Sub-tropical Monsoon
CH2	The valley plain area of Wuming Basin	Sub-tropical Monsoon
CH3	The valley plain area of Wuming Basin	Sub-tropical Monsoon
CH4	The lower hilly and wide valley basin of Dehong	Sub-tropical Monsoon
CH5	The low mountain and hilly area in Lufeng Basin	Sub-tropical Monsoon
CH6	The lower hilly and wide valley basin of Ganzhou	Sub-tropical Monsoon
CH7	The lower hilly and wide valley basin of Guiyang	Sub-tropical Monsoon
CH8	The lower hilly and wide valley basin of Qiandongnan	Sub-tropical Monsoon
CH9	The lower hilly and wide valley basin of Sanming	Sub-tropical Monsoon
CH10	The lower hilly and wide valley basin of Ji'an	Sub-tropical Monsoon
CH11	The lower hilly and wide valley basin of Zunyi	Sub-tropical Monsoon
CH12	The valley plain area of Xinjiang Basin	Sub-tropical Monsoon
CH13	The low-lying land of lakeshore plain of Dongting Lake	Sub-tropical Monsoon
CH14	The first grade terrace of Xinlixi River in the valley plain area of Jinqu Basin, Eastern China	Sub-tropical Monsoon
CH15	The alluvial and lacustrine plain area of Jianghan Plain, Central China	Sub-tropical Monsoon

CH16	The alluvial-marine plain area in North Zhejiang Plain, Eastern China	Sub-tropical Monsoon
CH17	The alluvial-marine plain area of the Yangtze River Delt	Sub-tropical Monsoon
CH18	The hilly and low-lying area of Zhenjiang in Jiangsu Province, Eastern China	Sub-tropical Monsoon
CH19	The first grade terrace in the valley plain of QingYijiang River	Sub-tropical Monsoon
CH20	The low-lying land of lakeshore plain of Chaohu Lake in Anhui Province, Eastern China	Sub-tropical Monsoon
CH21	The low foothill area of Xinyang in southern margin of North China Plain	Sub-tropical Monsoon
CH22	The first grade terrace of Bao River in alluvial and lacustrine plain area of the Hanzhong Basin, in southern Shaanxi Province, China	Sub-tropical Monsoon
CH23	The alluvial-marine plain area of Yancheng in North Jiangsu Plain, Eastern China	Sub-tropical Monsoon
CH24	The alluvial and lacustrine plain area of Xuzhou in North China Plain	Temperate Monsoon
CH25	The coastal plain area in North Jiangsu Plain, Eastern China	Temperate Monsoon
CH26	The low-lying land of lakeshore plain of Weishan Lake in North China Plain	Temperate Monsoon
CH27	The first grade terrace of the Yellow River in Yinchuan Plain, Northwest China	Temperate Continental
CH28	The coastal plain area in Liaohe Plain, Northeast China	Temperate Monsoon
CH29	The first grade terrace of East Liao River in Liaohe Plain, Northeast China	Temperate Monsoon
CH30	The interchannel zone between Lalin River and Mangniu River in Song Nen Plain, Northeast China	Temperate Monsoon
CH31	The first grade terrace of Songhua River in Sanjiang Plain, Northeast China	Temperate Monsoon

Table S5c | Basic soil chemistry of the 31 paddy soils sampled in China.

No.	soil pH	CEC[a]	Clay	SOC[b]	Total As	Chalcophile metals				HCl-extractable Fe	Total zerovalent sulfur[c]	
						Cd	Pb	Cu	Zn		control	3 mmol/kg sulfate
		cmol/kg	%	g/kg	mg/kg					mmol/kg	mmol/kg	
CH1	5.1	4.0	16.5	27.9	6.7	0.1	9.9	3.3	35.3	31.9	0.4	1.5
CH2	5.6	9.2	20.3	56.5	34.2	0.3	33.3	15.7	82.3	74.7	0.9	1.9
CH3	6.1	8.2	24.4	36.7	15.5	0.6	23.2	28.5	108.4	94.6	0.2	0.7
CH4	6.2	9.2	33.0	25.9	5.9	0.1	24.6	11.7	87.3	84.1	2.2	2.2
CH5	6.9	20.0	29.8	61.6	8.2	0.7	25.3	74.4	103.4	113.3	0.6	1.9
CH6	4.9	5.5	14.7	20.7	38.8	0.4	53.9	36.7	111.3	78.1	0.0	0.7
CH7	6.9	15.7	13.2	104.4	15.5	0.5	26.6	31.0	142.8	69.7	0.1	1.2
CH8	5.8	8.2	37.5	39.7	10.3	0.2	21.1	17.5	83.7	30.0	0.2	1.3
CH9	5.3	4.2	9.6	42.9	2.6	0.2	31.7	20.0	126.4	41.5	0.3	0.7
CH10	4.9	5.6	17.0	25.5	8.4	0.1	19.1	14.0	63.8	106.3	0.2	0.9
CH11	8.0	16.6	28.6	46.8	11.1	0.6	23.0	25.3	100.1	99.4	0.7	0.8
CH12	4.5	4.2	18.5	39.3	7.5	0.6	19.7	74.3	52.8	60.4	0.1	1.2
CH13	5.6	9.8	17.0	14.0	15.9	0.3	29.9	21.3	89.3	129.1	0.2	1.0

CH14	5.5	10.9	16.9	21.4	8.0	0.2	23.2	7.9	57.4	57.2	0.3	0.9
CH15	8.1	11.8	11.4	25.7	12.4	0.3	22.3	30.9	110.2	130.2	0.9	1.7
CH16	6.4	16.6	43.2	35.8	6.1	0.2	24.6	24.4	79.7	98.1	0.2	1.8
CH17	7.0	18.3	31.1	33.7	11.0	0.2	22.8	26.6	110.5	110.7	0.2	0.8
CH18	7.2	9.7	16.6	28.2	7.9	0.1	18.7	16.9	58.9	110.3	0.6	1.5
CH19	5.0	10.7	24.8	34.5	9.9	0.2	23.6	14.3	62.0	90.3	0.8	1.2
CH20	5.7	15.7	20.6	27.6	7.0	0.1	14.8	12.5	44.1	99.5	0.4	1.3
CH21	5.4	10.4	18.3	34.3	5.8	0.1	16.3	12.7	55.4	132.1	0.5	1.2
CH22	5.5	12.9	21.0	38.8	9.5	0.3	20.4	19.5	77.6	142.3	0.6	1.8
CH23	6.2	6.4	25.1	33.3	5.9	0.1	15.0	13.5	67.4	105.7	0.2	1.3
CH24	7.7	15.6	13.1	32.5	11.8	0.2	16.9	19.5	76.2	115.1	1.3	2.3
CH25	8.9	16.3	28.3	27.2	16.5	0.2	27.9	27.1	119.6	120.4	1.4	1.6
CH26	7.7	17.9	28.7	42.7	13.0	0.3	35.0	23.3	83.1	113.9	1.9	2.6
CH27	8.5	4.7	10.6	17.9	11.3	0.2	12.4	15.8	61.9	79.2	2.4	3.1
CH28	7.2	20.6	15.8	28.4	7.9	0.1	17.9	18.1	71.4	69.5	2.0	2.8
CH29	6.7	16.6	13.8	30.4	8.6	0.1	15.4	16.9	67.2	130.5	2.0	2.3
CH30	6.3	18.8	25.1	45.1	9.6	0.1	17.3	19.9	68.3	146.3	0.2	1.1
CH31	5.9	19.0	25.3	39.5	10.0	0.1	14.9	14.0	44.8	184.7	0.3	1.0

[a] Cation exchange capacity; [b] Soil organic carbon; [c] Total zerovalent sulfur formation after 14 days of soil incubation as described in section 4, which was calculated as sum of aqueous and solid phase zerovalent sulfur for control treatments and 3 mmol/kg sulfate addition treatments, respectively.

Table S6 | Spearman's correlation analyses for soil and pore water parameters for anaerobic soil incubations of 31 paddy soils from China and 2 paddy soils from Italy; marked in green are R values with a P-value < 0.05

R (control, no S)	methylated thioarsenates [%]	total thiolation [%]	soil pH	soil-bound zerovalent S [µmol/kg]	HCl-extractable Fe [g/kg]	soil total As [mg/kg]	soil organic carbon [g/kg]	CEC [cmol/kg]	Clay [%]	Total chalcophile metals [mmol/kg]	porewater pH	methylated oxyarsenates [%]	porewater zerovalent S [µmol/l]	porewater As [µg/L]	porewater Fe [mg/L]
inorganic thioarsenates [%]	0.22	0.85	0.58	0.46	-0.10	-0.18	-0.10	0.17	-0.25	-0.04	0.44	-0.01	0.25	-0.48	-0.89
methylated thioarsenates [%]		0.54	-0.31	-0.21	-0.36	-0.63	0.19	-0.01	0.00	-0.17	-0.46	0.69	0.03	-0.63	-0.04
total thiolation [%]			0.28	0.30	-0.21	-0.34	0.02	0.06	-0.33	-0.16	0.16	0.29	0.26	-0.58	-0.66
soil pH				0.54	0.33	0.32	0.06	0.54	0.08	0.21	0.87	-0.54	-0.03	-0.12	-0.79
soil-bound zerovalent S [µmol/kg]					0.28	0.10	-0.04	0.30	-0.09	-0.16	0.69	-0.19	0.31	-0.24	-0.51
HCl-extractable Fe [g/kg]						0.27	0.00	0.54	0.16	-0.09	0.37	-0.31	-0.09	0.24	0.02
soil total As [mg/kg]							0.00	0.12	-0.07	0.46	0.37	-0.56	-0.33	0.45	0.02
soil organic carbon [g/kg]								0.30	0.36	0.32	0.04	0.12	-0.02	-0.24	0.06
CEC [cmol/kg]									0.37	0.08	0.57	-0.17	0.08	0.00	-0.33
Clay [%]										0.10	0.05	0.22	-0.16	-0.09	0.13

Total chalcophile metals [mmol/kg]											0.23	-0.27	-0.26	-0.15	-0.16
porewater pH												-0.59	0.17	-0.02	-0.71
methylated oxyarsenates [%]													0.07	-0.41	0.23
porewater zerovalent S [µmol/L]														0.06	-0.20
porewater As [µg/L]															0.33

P-Value (control, no S)	methylated thioarsenates [%]	total thiolation [%]	soil pH	soil-bound zerovalent S [µmol/kg]	HCl-extractable Fe [g/kg]	soil total As [g/kg]	soil organic carbon [g/kg]	CEC [cmol/kg]	Clay [%]	Total chalcophile metals [mmol/kg]	porewater pH	methylated oxyarsenates [%]	porewater zerovalent S [µmol/l]	porewater As [µg/L]	porewater Fe [mg/L]
inorganic thioarsenates [%]	0.22	0.00	0.00	0.01	0.57	0.32	0.58	0.35	0.17	0.85	0.01	0.97	0.17	0.01	0.00
methylated thioarsenates [%]		0.00	0.08	0.23	0.04	0.00	0.30	0.95	1.00	0.36	0.01	0.00	0.86	0.00	0.85
total thiolation [%]			0.11	0.09	0.24	0.05	0.93	0.75	0.07	0.39	0.38	0.10	0.15	0.00	0.00
soil pH				0.00	0.06	0.07	0.74	0.00	0.69	0.26	0.00	0.00	0.89	0.52	0.00
soil-bound zerovalent S [µmol/kg]					0.12	0.56	0.82	0.10	0.64	0.38	0.00	0.29	0.08	0.20	0.00

HCl-extractable Fe [g/kg]						0.14	0.98	0.00	0.40	0.64	0.04	0.07	0.62	0.19	0.91
soil total As [mg/kg]							1.00	0.52	0.72	0.01	0.04	0.00	0.06	0.01	0.90
soil organic carbon [g/kg]								0.10	0.05	0.08	0.85	0.50	0.93	0.20	0.75
CEC [cmol/kg]									0.04	0.65	0.00	0.37	0.68	1.00	0.07
Clay [%]										0.60	0.79	0.23	0.38	0.61	0.49
Total chalcophile metals [mmol/kg]											0.22	0.15	0.16	0.42	0.40
porewater pH												0.00	0.36	0.92	0.00
methylated oxyarsenates [%]													0.69	0.02	0.19
porewater zerovalent S [µmol/L]														0.74	0.25
porewater As [µg/L]															0.07

R (Sulfate Treatment)	methylated thioarsenates [%]	total thiolation [%]	soil pH	soil-bound zerovalent S [µmol/kg]	HCl-extractable Fe [g/kg]	soil total As [mg/kg]	soil organic carbon [g/kg]	CEC [cmol/kg]	Clay [%]	Total chalcophile metals [mmol/kg]	porewater pH	methylated oxyarsenates [%]	porewater zerovalent S [µmol/l]	porewater As [µg/L]	porewater Fe [mg/L]
inorganic	0.08	0.91	0.59	0.35	-0.07	-0.14	-0.16	0.18	-0.17	-0.03	0.63	-0.06	-0.19	-0.39	-0.86

thioarsenates [%]														
methylated thioarsenates [%]	0.40	-0.41	-0.33	-0.35	-0.67	0.21	-0.02	0.02	-0.21	-0.34	0.72	-0.13	-0.46	0.27
total thiolation [%]	0.38	0.21	-0.22	-0.34	-0.06	0.11	-0.20	-0.11	0.52	0.18	-0.23	-0.50	-0.73	
soil pH	0.49	0.33	0.32	0.06	0.54	0.08	0.21	0.66	-0.47	-0.07	-0.05	-0.90		
soil-bound zerovalent S [µmol/kg]	0.21	0.12	-0.04	0.25	-0.04	-0.15	0.44	-0.30	0.25	-0.26	-0.54			
HCl-extractable Fe [g/kg]	0.26	0.00	0.54	0.15	-0.09	0.39	-0.38	0.07	0.29	-0.07				
soil total As [mg/kg]	0.00	0.12	-0.07	0.46	0.09	-0.67	-0.17	0.47	-0.08					
soil organic carbon [g/kg]	0.30	0.36	0.32	-0.15	0.09	0.05	-0.21	-0.01						
CEC [cmol/kg]	0.37	0.08	0.38	-0.26	0.11	0.07	-0.39							
Clay [%]	0.10	-0.18	0.17	0.25	-0.09	0.11								
Total chalcophile metals [mmol/kg]	-0.02	-0.22	-0.12	-0.14	-0.16									
porewater pH	-0.36	-0.03	-0.04	-0.69										
methylated oxyarsenates [%]	-0.14	-0.46	0.34											
porewater zerovalent S [µmol/L]	-0.04	0.03												
porewater As [µg/L]	0.34													

P-Value (Sulfate Treatment)	methylated thioarsenates [%]	total thiolation [%]	soil pH	soil-bound zerovalent S [µmol/kg]	HCl-extractable Fe [g/kg]	soil total As [mg/kg]	[g/kg]	CEC [cmol/kg]	Clay [%]	Total chalcophile metals [mmol/kg]	porewater pH	methylated oxyarsenates [%]	porewater zerovalent S [µmol/l]	porewater As [µg/L]	porewater Fe [mg/L]
inorganic thioarsenates [%]	0.65	0.00	0.00	0.04	0.68	0.44	0.37	0.34	0.35	0.86	0.00	0.74	0.28	0.03	0.00
methylated thioarsenates [%]		0.02	0.02	0.06	0.05	0.00	0.25	0.90	0.90	0.26	0.06	0.00	0.46	0.01	0.16
total thiolation [%]			0.03	0.23	0.22	0.05	0.73	0.56	0.27	0.56	0.00	0.32	0.20	0.00	0.00
soil pH				0.00	0.06	0.07	0.74	0.00	0.69	0.26	0.00	0.01	0.68	0.79	0.00
soil-bound zerovalent S [µmol/kg]					0.25	0.49	0.81	0.18	0.82	0.41	0.01	0.09	0.16	0.15	0.00
HCl-extractable Fe [g/kg]						0.14	0.99	0.00	0.41	0.62	0.03	0.03	0.71	0.12	0.72
soil total As [mg/kg]							1.00	0.52	0.72	0.01	0.65	0.00	0.33	0.01	0.69
soil organic carbon [g/kg]								0.10	0.05	0.08	0.41	0.63	0.77	0.27	0.95
CEC [cmol/kg]									0.04	0.65	0.03	0.16	0.56	0.71	0.04
Clay [%]										0.60	0.33	0.36	0.17	0.64	0.57

Total chalcophile metals [mmol/kg]	0.89	0.23	0.51	0.46	0.41
porewater pH		0.05	0.87	0.82	0.00
methylated oxyarsenates [%]			0.42	0.01	0.08
porewater zerovalent S [µmol/L]				0.81	0.88
porewater As [µg/L]					0.07

Table S7 | Relative importance of predictor values for the occurrence of inorganic and methylated thioarsenates (%) using multiple linear regression analysis with soil physical and chemical properties separated by control (no S) and sulfate-addition (S) incubations; for methylated thioarsenates two models were used, one including the share of methylated oxyarsenates in the pore water and one only using soil parameters; significance levels (sig. level) are indicated as *** (0-0.001), ** (0.001-0.01), * (0.01-0.05), and . (0.1-1)

Control (no S)	**weight factor %**	**lower 95% range [%]**	**upper 95% range [%]**	**sig. level**
inorganic thioarsenates				
CEC [cmol/kg]	13.6	1.7	30.2	**
Clay [%]	-18.3	-3.3	-40.6	**
HCl-extractable Fe [g/kg]	-6	-1.1	-16.6	*
{H+} [mol/L]	-4.4	-2.8	-14.5	
zerovalent S [µmol/kg]	50.8	17.8	74.9	***
SOC [g/kg]	-4.5	-0.9	-11.2	
total soil As [mg/kg]	-1.3	-0.4	-8.1	
Total chalcophile metals [mmol/kg]	-1.1	-0.5	-8.2	
$r^2 = 0.7352$, $p = 7.1*10^{-5}$				
methylated thioarsenates + oxyarsenates				
CEC [cmol/kg]	**3.2**	1.6	24.5	
Clay [%]	-9.8	-1.1	-21.6	*
HCl-extractable Fe [g/kg]	-10.8	-3.3	-29.1	
{H+} [mol/L]	-1.8	-0.9	-10.9	
zerovalent S [µmol /kg]	-3.2	-0.8	-20.4	
SOC [g/kg]	-0.8	-0.7	-9.4	
total soil As [mg/kg]	-18.8	-8.8	-30.3	*
Total chalcophile metals [mmol/kg]	5.7	2.3	23	*
methylated oxyarsenates [%]	45.9	8.2	55.7	**

$r^2 = 0.6902$, $p = 8.9*10^{-4}$

methylated thioarsenates - oxyarsenates				
CEC [cmol/kg]	-6	-1.6	-25.7	
Clay [%]	-10.1	-1	-23.8	.
HCl-extractable Fe [g/kg]	-26.9	-3.9	-45.4	*
{H+} [mol/L]	-4	-1.3	-19.6	
zerovalent S [µmol /kg]	-6.7	-0.9	-30.3	
SOC [g/kg]	-1	-0.8	-15.6	
total soil As [mg/kg]	-40.4	-12.3	-49.1	**
Total chalcophile metals [mmol/kg]	4.9	2.6	37.1	
$r^2 = 0.5022$, $p = 2.8*10^{-2}$				

Sulfate treatment	**weight factor %**	**lower 95% range [%]**	**upper 95% range [%]**	**sig. level**
inorganic thioarsenates				
CEC [cmol/kg]	20.6	3	30.6	**
Clay [%]	-12.6	-1.6	-31.5	*
HCl-extractable Fe [g/kg]	-8.8	-1.8	-19.4	*
{H+} [mol/L]	-4.2	-2.7	-17.3	
zerovalent S [µmol /kg]	46.1	21	68.6	**
SOC [g/kg]	-6.3	-1.1	-15.5	*
total soil As [mg/kg]	-0.8	-0.4	-10.4	
Total chalcophile metals [mmol/kg]	-0.8	-0.5	-7.7	
$r^2 = 0.674$, $p = 5.6*10^{-4}$				

methylated thioarsenates + oxyarsenates

CEC [cmol/kg]	4.3	1.5	14.6	
Clay [%]	-1.5	-0.5	-17.5	
HCl-extractable Fe [g/kg]	-12.9	-3.2	-21	
{H+} [mol/L]	-0.8	-0.5	-15.4	
zerovalent S [µmol /kg]	-3.7	-0.6	-13.6	
SOC [g/kg]	-0.3	-0.4	-8.2	
total soil As [mg/kg]	-11.2	-4.7	-23.6	
Total chalcophile metals [mmol/kg]	1.5	0.6	19.9	
methylated oxyarsenates [%]	63.8	21.2	65.8	***
$r^2 = 0.8304$, $p = 2.8*10^{-6}$				

methylated thioarsenates - oxyarsenates				
CEC [cmol/kg]	-8.3	-1.8	-19.6	
Clay [%]	-1.9	-0.6	-29.4	
HCl-extractable Fe [g/kg]	-39.1	-3.6	-47.3	*
{H+} [mol/L]	-1.7	-1.2	-27.5	
zerovalent S [µmol /kg]	-10.9	-0.9	-28	.
SOC [g/kg]	-0.8	-0.8	-14.9	
total soil As [mg/kg]	-33.1	-9.3	-49.7	*
Total chalcophile metals [mmol/kg]	4.1	1.1	40.9	
$r^2 = 0.5151$, $p = 2.2*10^{-2}$				

Note: Implications of HCl-extractable Fe, pH, zerovalent S, total soil As, and methylated oxyarsenates are discussed in the main manuscript; the reasons for the sig. negative impact of clay on both inorganic and methylated thioarsenates and the sig. positive impact of CEC (Cation Exchange Capacity) on inorganic thioarsenates are currently unclear. The correlation with CEC might be in line with previous observations of high ionic strengths increasing the kinetics of inorganic thioarsenate formation from arsenite and reduced sulfur in solution. [11, 12]

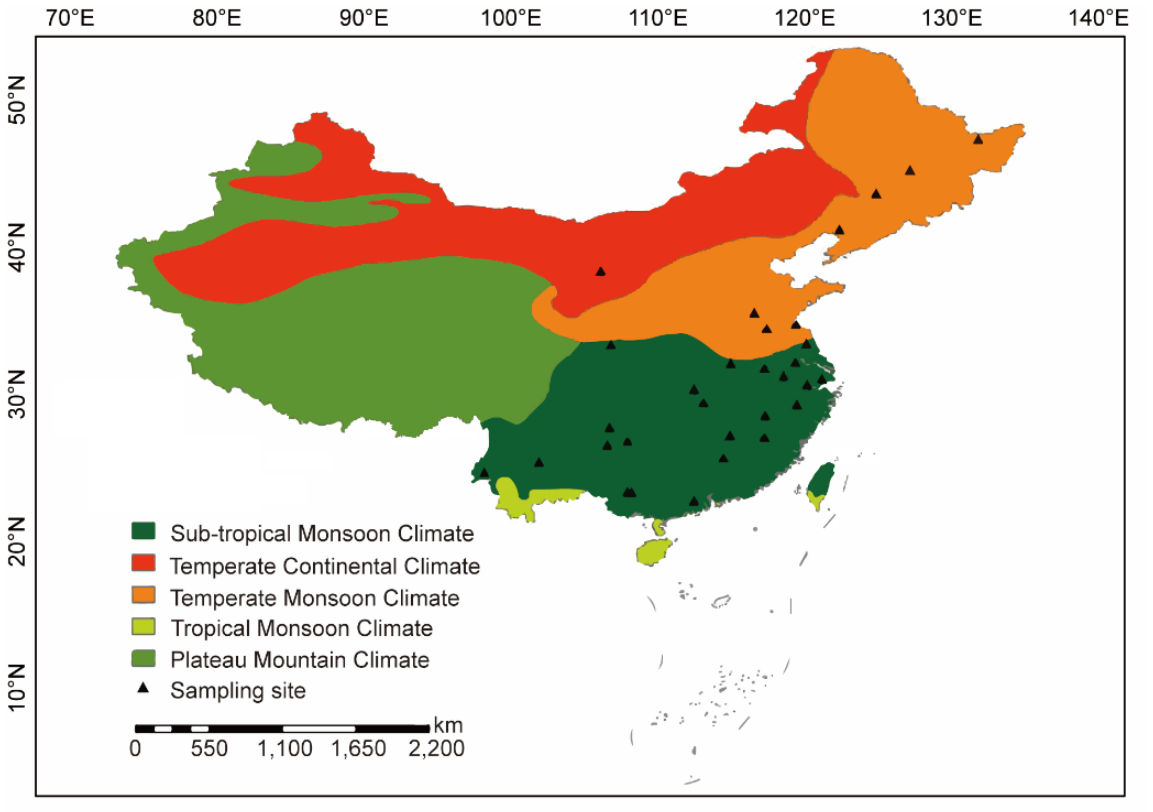

Figure S8 | Sampling sites of 31 paddy fields in different climate zones over China. The geographic origins covered an area from 22.5° to 47.2° N and 98.4° to 131.6° E, spanning climate zones from sub-tropical monsoon climate (23 fields) to temperate continental climate (1 fields) and temperate monsoon climate (7 fields).The base map used is from the National Fundamental Geographic Information System of China.

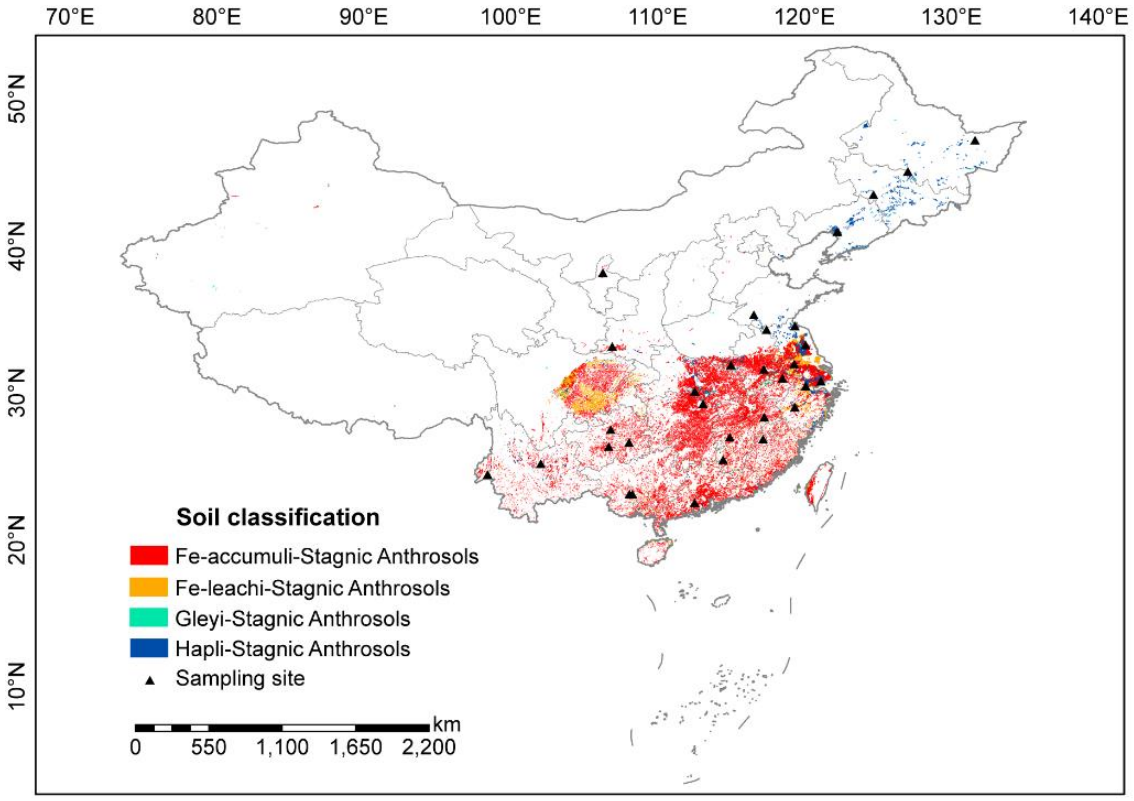

Figure S9 | Sampling sites of 31 paddy fields based on soil classification over China. The colored background indicates the distribution of Stagnic Anthrosols in China. Based on Chinese Soil Taxonomic Classification (adopted by WRB in 1998), all paddy soils used here are classified as Stagnic Anthrosols, including Fe-accumuli- (15 soils), Fe-leachi-(8 soils), Hapli- (8 soils) Stagnic Anthrosols. Stagnic Anthrosols are anthrosols that have an anthrostagnic moisture regime and have both a hydragric epipedon (including a ultivated horizon and a plowpan) and a hydragric horizon. The base map used is from the National Fundamental Geographic Information System of China.

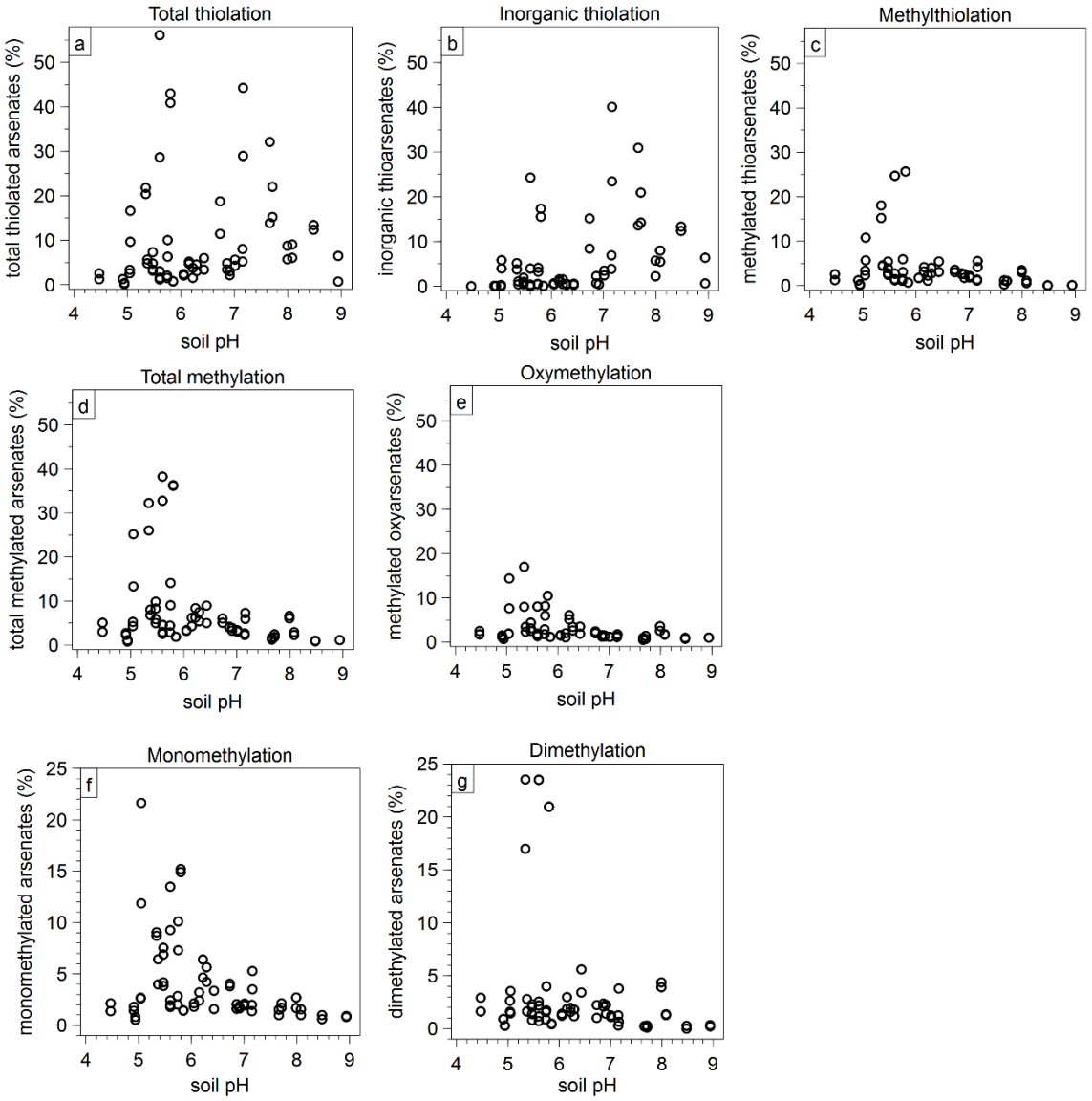

Figure S10 | Summarized As speciation determined in anaerobic soil incubations in relation to soil pH. Data from control and sulfate addition for 31 paddy soils from China and 2 paddy soils from Italy were combined. a) total thiolation which is the sum of b) inorganic thiolation and c) methylthiolation; d) total methylation which is the sum of e) oxymethylation and c) methylthiolation; f) all mono- and g) all dimethylated arsenates (integrating oxy and thio species).

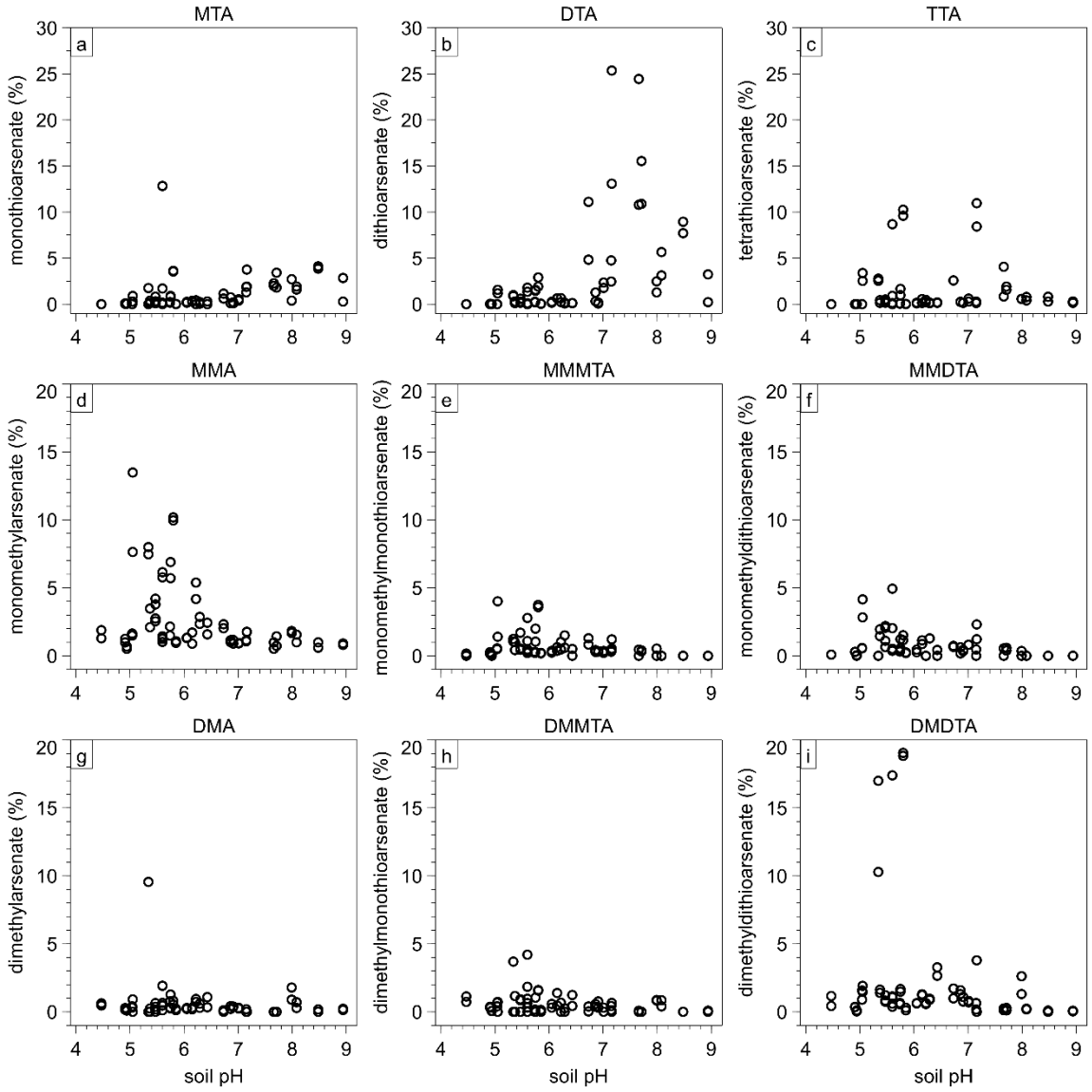

Figure S11 | Individual As speciation of inorganic thioarsenates in anaerobic soil incubations in relation to soil pH. a) MTA, b) DTA, c) TTA, d) monomethylated oxy- (MMA) and thioarsenates e) MMMTA, f) MMDTA) and g) dimethylated oxy- (DMA), and thioarsenates h) DMMTA, i) DMDTA .Data from control and sulfate addition for 31 paddy soils from China and 2 paddy soils from Italy were combined.

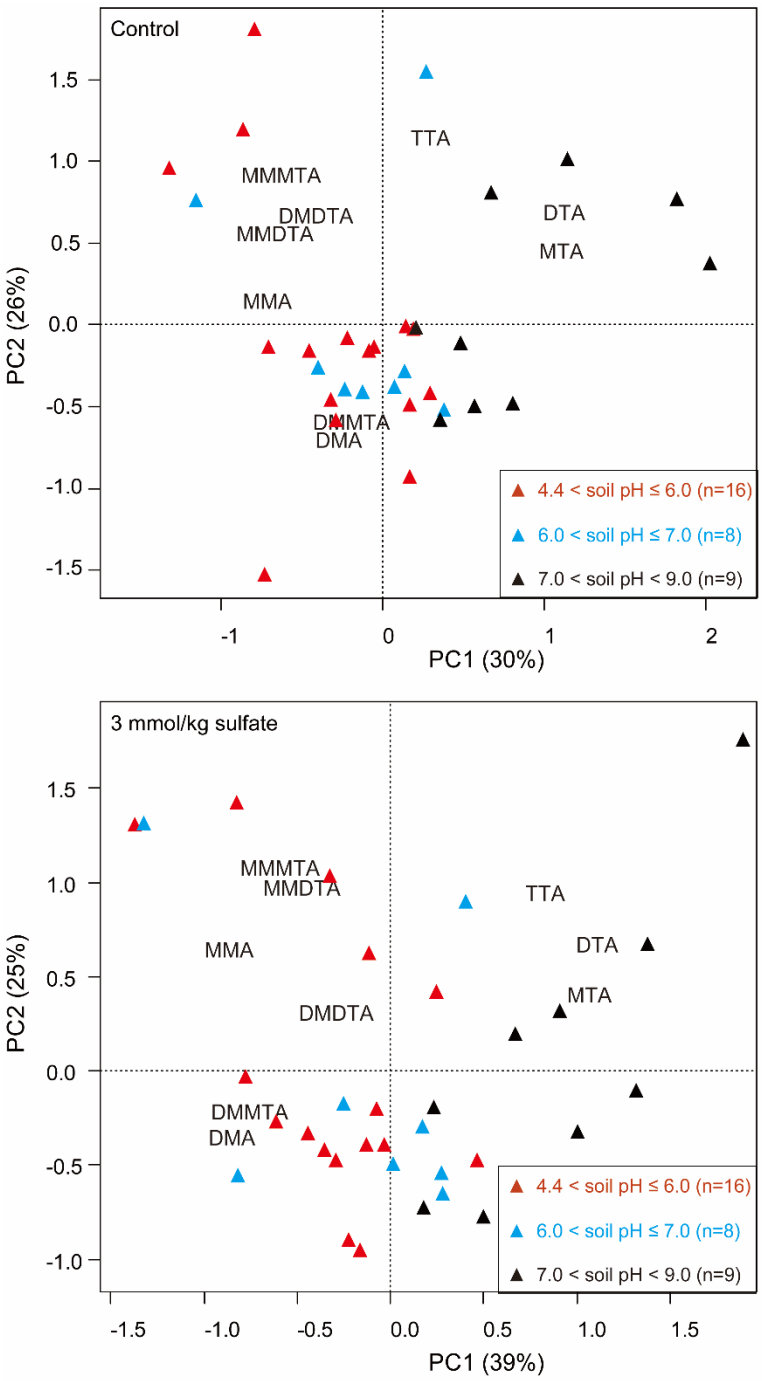

Figure S12 | Principal component analysis of As speciation in anaerobic soil incubations. Site distribution reveals clustering of methylated oxyarsenates (DMA and MMA) and methylated thioarsenates (DMDTA, MMDTA, MMMTA, DMMTA) with low pH soils and inorganic thioarsenates (MTA, DTA, and TTA) with high pH soils during anaerobic incubation of 31 paddy soils from China and 2 paddy soils from Italy; a) control treatment and b) sulfate addition.

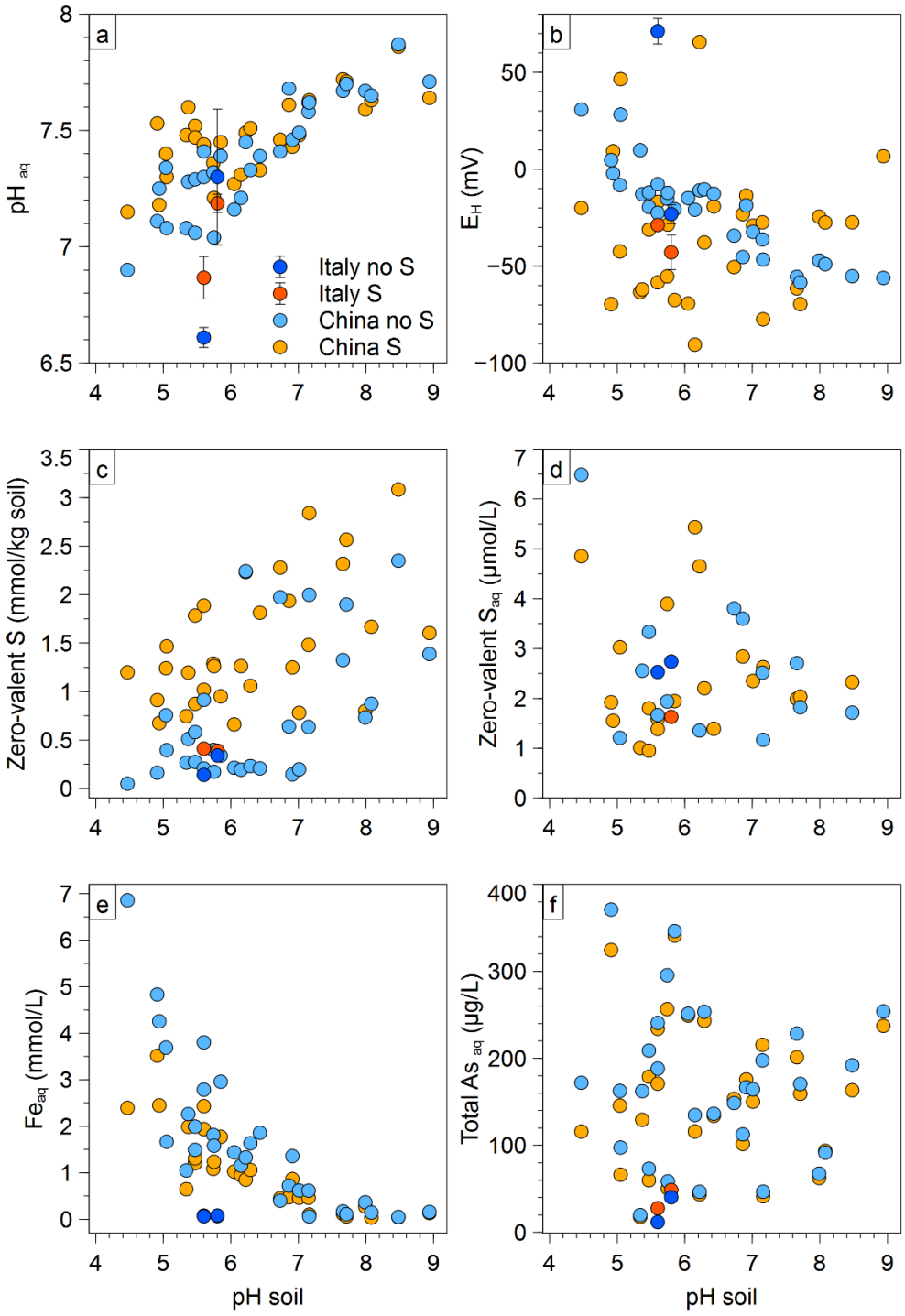

Figure S13 | Pore-water chemistry for anaerobic soil incubations as a function of soil pH. a) pore-water pH, b) E_H, c) solid phase zero-valent S, d) aqueous zero-valent S, e) total dissolved Fe, and f) total dissolved As for anaerobic soil incubations of 31 paddy

soils from China and 2 paddy soils from Italy (experimental triplicates); blue colors refer to control treatments (no S), orange-red colors to sulfate addition (S).

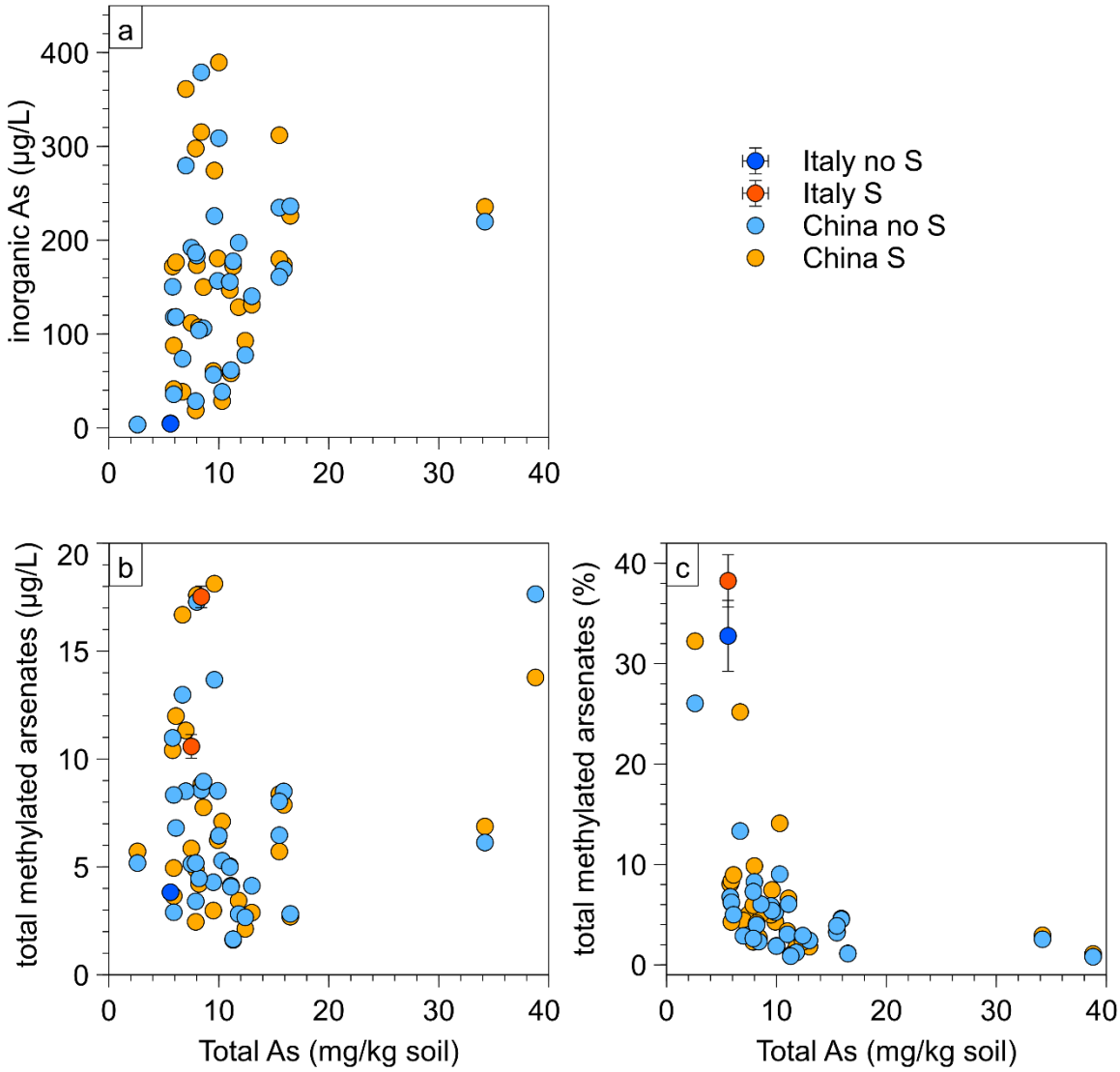

Figure S14 | Absolute and relative concentrations of inorganic As (a, b) and methylated oxyarsenates (c, d) in relation to total soil As. Anaerobic soil incubations were conducted with 31 paddy soils from China and 2 paddy soils from Italy (experimental triplicates); blue colors refer to control treatments (no S), orange-red colors to sulfate addition (S).

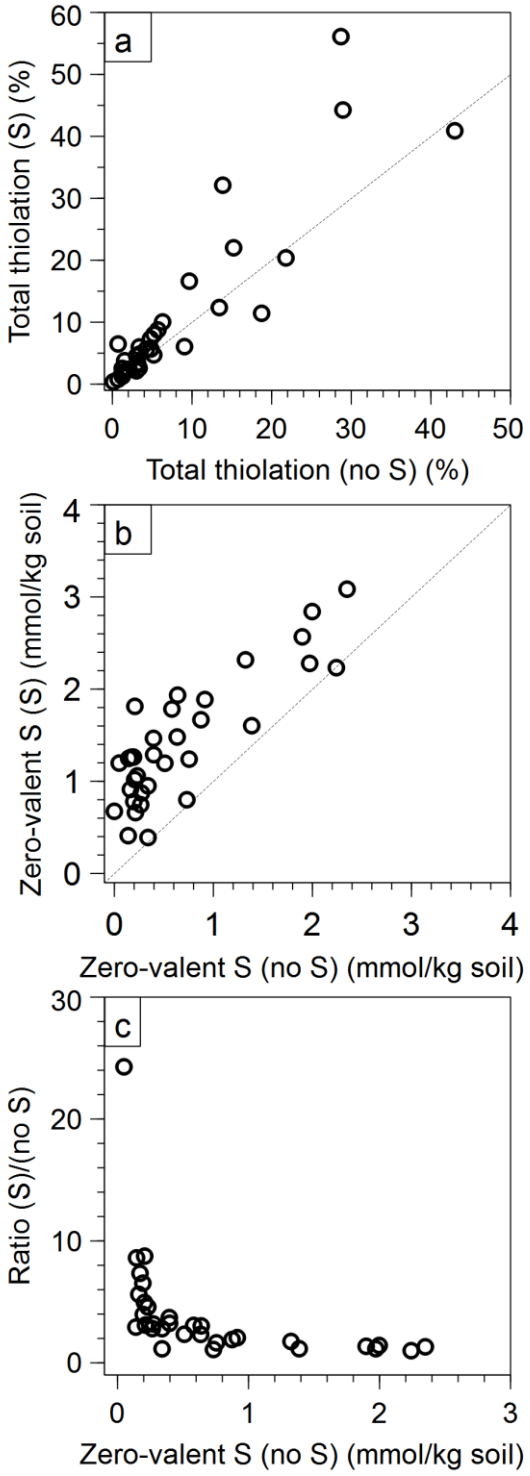

Figure S15 | Effects of sulfate addition on arsenic thiolation and zero-valent S formation. Comparison of a) total thiolation (%) and b) solid phase zero-valent S with and without sulfate addition; c) ratio of zero-valent S increase from control to sulfate-

treatment versus original zero-valent S concentrations in control for anaerobic soil incubations of 31 paddy soils from China and 2 paddy soils from Italy.

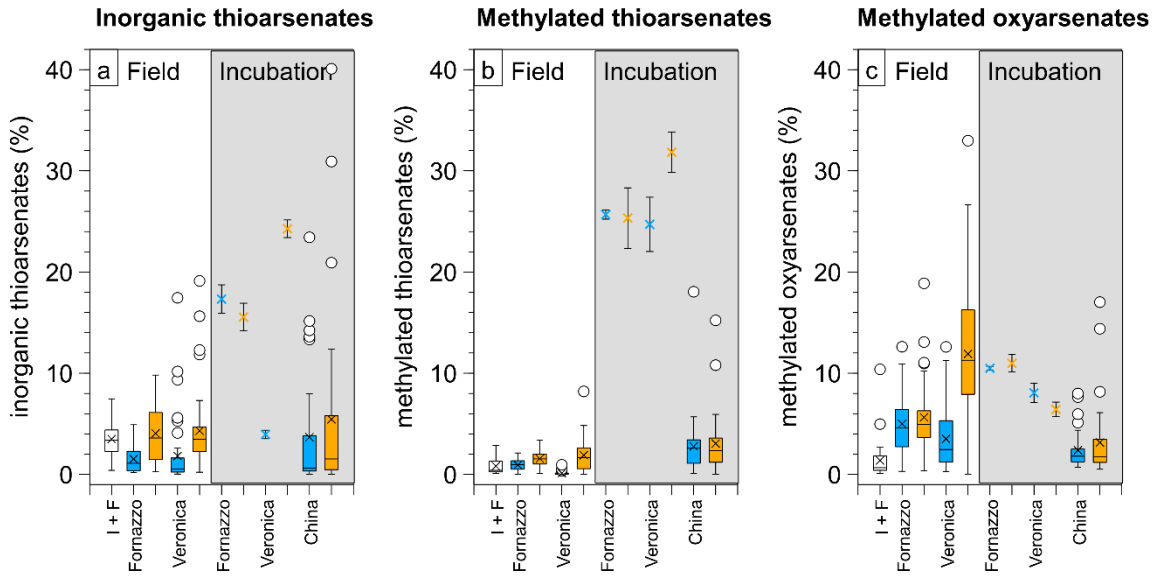

Figure S16 | Comparison of arsenic speciation in anaerobic soil incubations to mesocosm experiments and field survey. a) occurrence of inorganic thioarsenates, b) methylated thioarsenates, and c) methylated oxyarsenates in the field with plants (one-time survey Italy/France at late plant growth stage (I+F); n = 35; mesocosms with Veronica and Fornazzo soil integrated over whole rice cultivation period of 4 months; n = 42 each) and in anaerobic soil incubations (with Veronica and Fornazzo soils (n=3 each) and paddy soils over a pH-gradient in China (n=31 each); blue colors refer to control treatments (no S), orange colors to sulfate addition (S)

4. Methods

Table S8 | Quantitative Recovery of As species in a fresh model pore water sample spiked with 1 µg/L of DMA, DMMTA, arsenite, MMA, MMMTA, and arsenate, stabilized with 10 mM DTPA, and analyzed 1:5 and 1:10 diluted with deionized water using 2.4 % methanol in the eluent and either individual or averaged calibration

		DMA	DMMTA[a]	Arsenite	DMDTA[b]	MMA	MMMTA[c]	MMDTA[d]	Arsenate	MTA[e]	DTA[f]	Sum of As species
Counts per Selicond	DMA 1 µg/L Standard	1001699										
	MMA 1 µg/L Standard					815446						
	Arsenate 1 µg/L Standard								876310			
	sample 1:10 dilution	151318	164191	37415	14160	114871	62514	87301	252602	19856	13196	
	sample 1:5 dilution	309624	400192	104872	36697	247134	153063	185058	415801	23790	13544	
Concentration (µg/L)	sample 1:10 dilution (measured concentration)	0.15	0.16	0.04	0.02	0.14	0.08	0.10	0.29	0.02	0.02	
	sample 1:5 dilution	0.31	0.40	0.11	0.05	0.30	0.19	0.21	0.47	0.03	0.02	

	(measured concentration)											
	sample 1:10 dilution x 10 (final concentration by individual calibration)	1.51	1.64	0.37	0.17	1.41	0.77	1.00	2.88	0.23	0.15	10.85[g]

		DMA	**DMMTA[a]**	**Arsenite**	**DMDTA[b]**	**MMA**	**MMMTA[c]**	**MMDTA[d]**	**Arsenate**	**MTA[e]**	**DTA[f]**	**Sum of As species**
	sample 1:5 dilution x 5 (final concentration by individual calibration)	1.55	2.00	0.52	0.23	1.52	0.94	1.06	2.37	0.14	0.08	10.94[g]
	sample 1:10 dilution x 10 (final concentration by averaged calibration)	1.69	1.83	0.42	0.16	1.28	0.70	0.97	2.81	0.22	0.15	11.02[g]
	sample 1:5 dilution	1.72	2.23	0.58	0.20	1.38	0.85	1.03	2.32	0.13	0.08	11.14[g]

	x 5 (final concentration by averaged calibration)											
(%) of total As	sample 1:10 dilution	13.9%	15.1%	3.4%	1.6%	13.0%	7.1%	9.2%	26.6%	2.1%	1.4%	>2.5% well detectable
	sample 1:5 dilution	14.1%	18.3%	4.8%	2.1%	13.9%	8.6%	9.7%	21.7%	1.2%	0.7%	>1% well detectable

Table S9 | Characteristics of irrigation water for mesocosm rice cultivation experiments.

Parameters	Irrigation water
pH	7.7
Conductivity (µS/cm)	508
TIC (mg/L)[a]	17.5
TOC (mg/L)[b]	1.2
Cl^- (mg/L)	11.4
NO_3^- (mg/L)	1.11
NO_2^- (mg/L)	1.05
PO_4^{3-} (mg/L)	1.01
SO_4^{2-} (mg/L)	11.1
Si (mg/L)	8.9
Mn (µg/L)	1.5
Cu (µg/L)	2.6
Zn (µg/L)	16.5
As (µg/L)	6.4

[a] Total inorganic carbon; [b] Total organic carbon

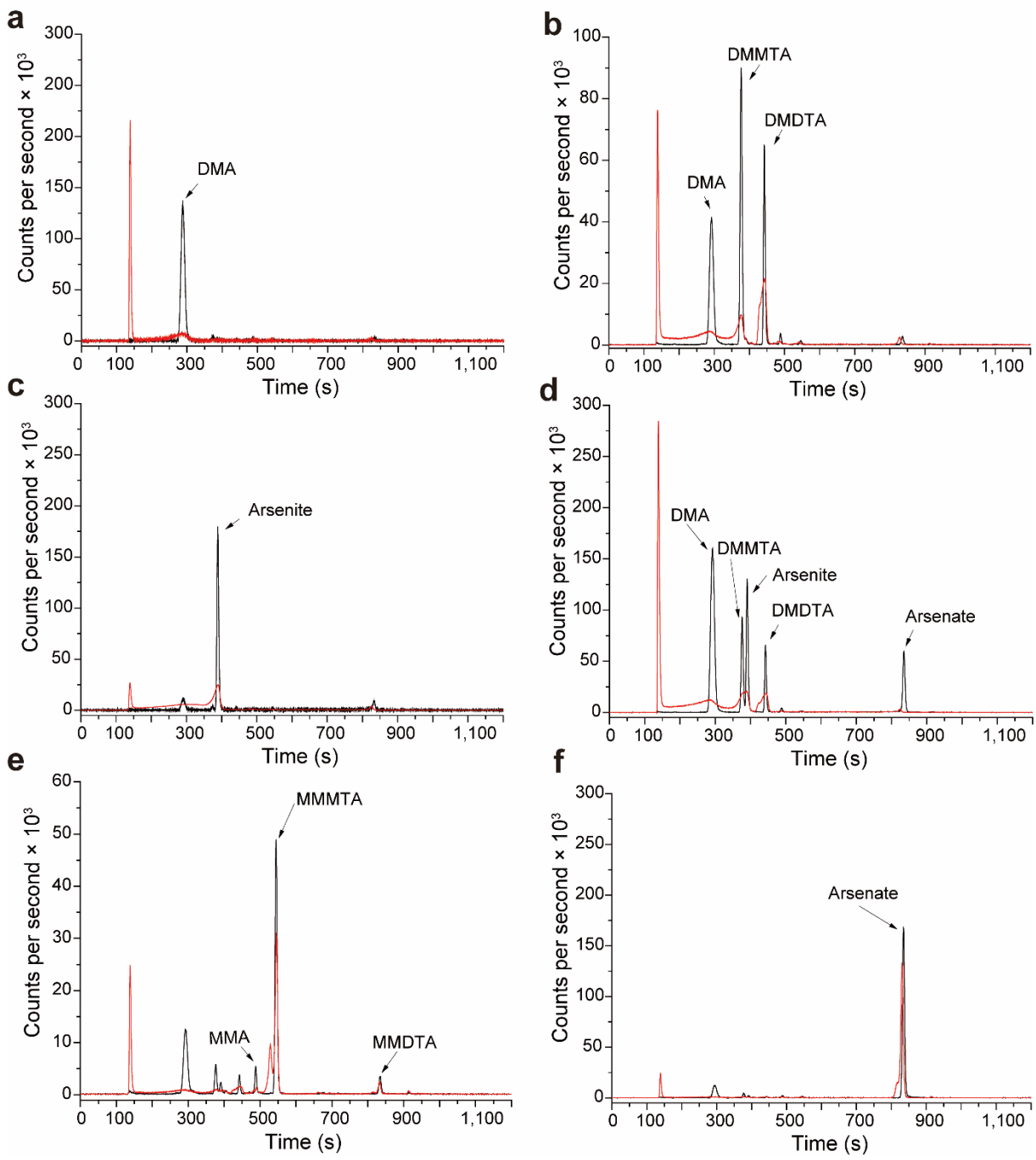

Figure S17 | Effect of 10 mM DTPA on retention time, peak shape, and resolution of As speciation. Tested model pore-water was spiked with 100 µg/L standards of a) DMA; b) DMMTA; c) arsenite; d) a mix of arsenite, DMA, DMMTA; e) MMMTA; f) arsenate; black lines = without DTPA, red lines = with 10 mM DTPA.

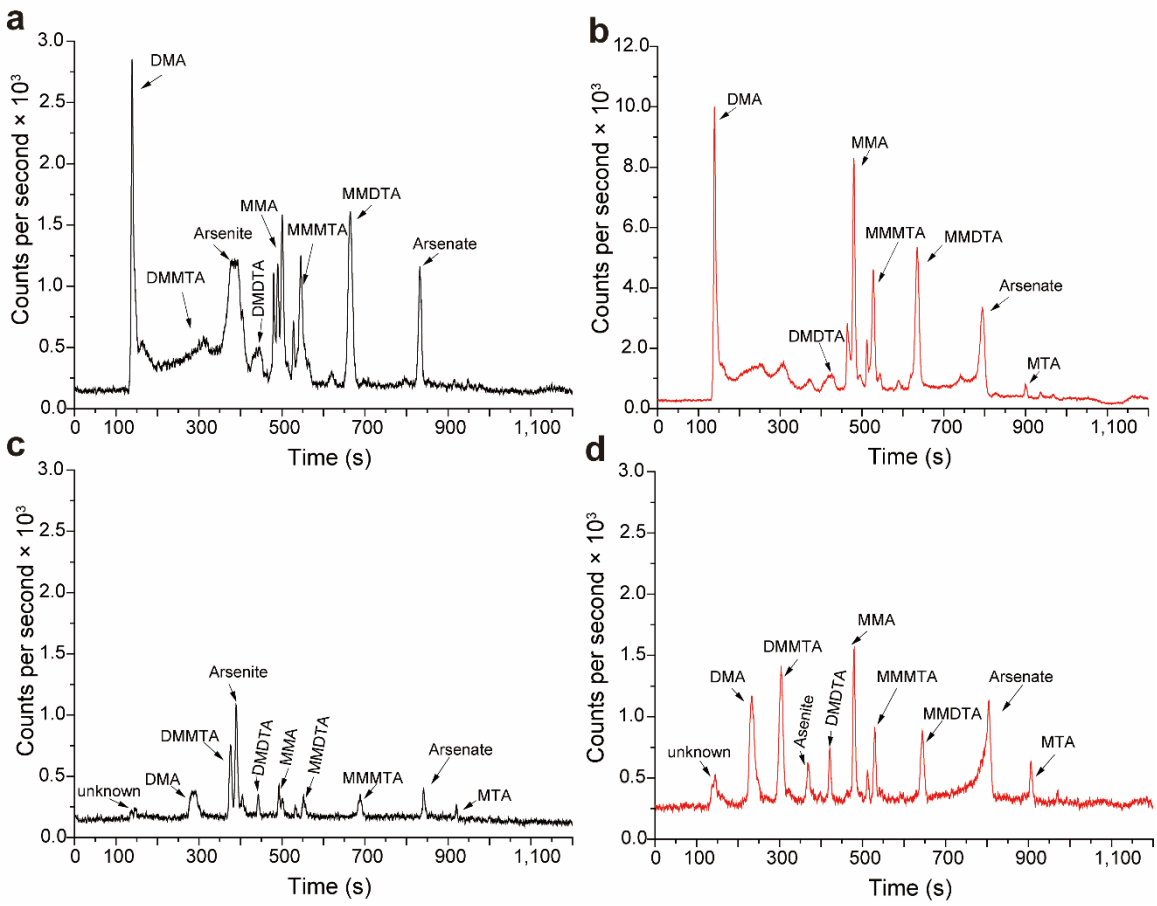

Figure S18 | Effect of sample dilution and use of methanol in the eluent on retention time, peak shape, and resolution of As speciation. Fresh, non-spiked model pore-water samples stabilized with 10 mM DTPAwere a) analyzed without dilution and without 2.4% methanol; b) analyzed without dilution with 2.4% methanol; c) diluted 1:10 with deionized water before analysis and analyzed without 2.4% methanol; d) diluted 1:10 with deionized water before analysis and analyzed with 2.4% methanol. All samples were analyzed with a 2.5-100 mM NaOH gradient eluent.

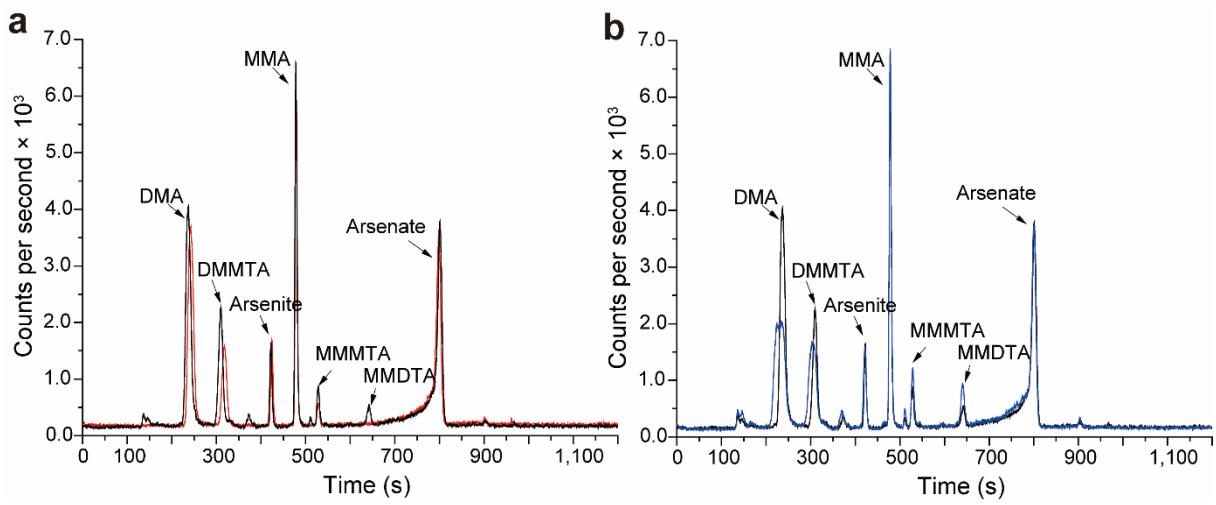

Figure S19 | Effect of pore-water matrix and different DTPA dilution on retention time, peak shape, and resolution of As speciation. Fresh model pore-water samples were spiked with 1 µg/L of DMA, DMMTA, arsenite, MMA, MMMTA, and arsenate,stabilized with 10 mM DTPA (all analyzed with 2.4% methanol in the eluent). a) comparison deionized water (red) and pore-water matrix 1:10 diluted (black), b) comparison 1:5 (blue) vs. 1:10 (black) dilution of pore-water matrix sample.

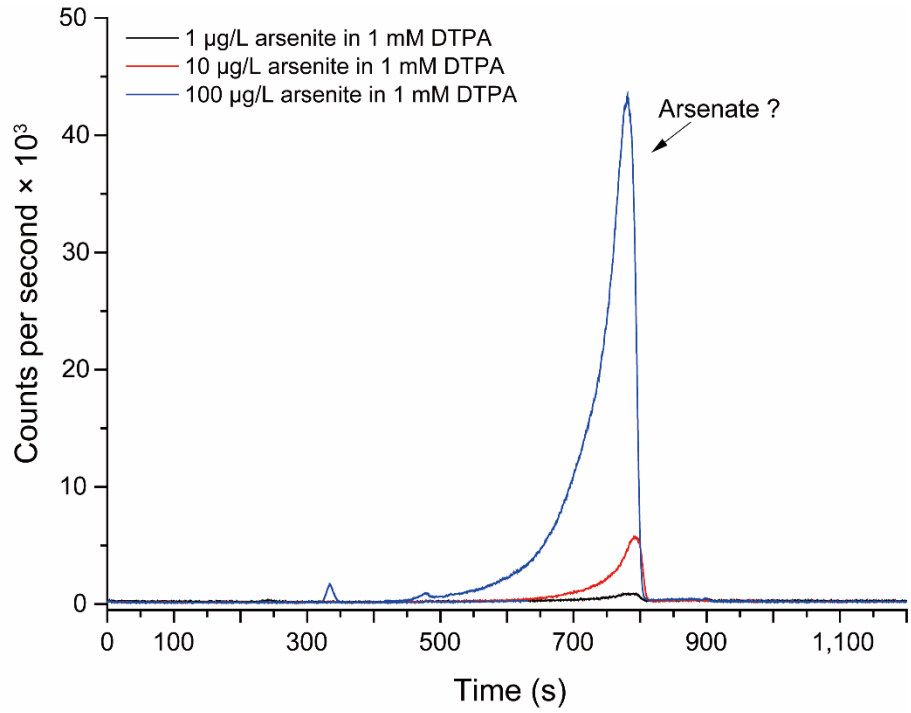

Figure S20 | Effect of 1 mM DTPA on arsenite standards in deionized water. The question mark behind the arsenate label indicates that the observed transformation product elutes at the retention time of arsenate but might also be an unidentified As-DTPA complex**.**

References

1. Samanta G, Clifford DA. Preservation of inorganic arsenic species in groundwater. *Environmental Science & Technology* 2005, **39**(22)**:** 8877-8882.

2. Planer-Friedrich B, London J, McCleskey RB, Nordstrom DK, Wallschläger D. Thioarsenates in geothermal waters of Yellowstone National Park: determination, preservation, and geochemical importance. *Environmental Science & Technology* 2007, **41**(15)**:** 5245-5251.

3. Kerl CF, Schindele RA, Brüggenwirth L, Colina Blanco AE, Rafferty C, Clemens S*, et al.* Methylated thioarsenates and monothioarsenate differ in uptake, transformation, and contribution to total arsenic translocation in rice plants. *Environmental Science & Technology* 2019, **53**(10)**:** 5787-5796.

4. Kerl CF, Rafferty C, Clemens S, Planer-Friedrich B. Monothioarsenate uptake, transformation, and translocation in rice plants. *Environmental Science & Technology* 2018, **52**(16)**:** 9154-9161.

5. Wallschläger D, London J. Determination of methylated arsenic-sulfur compounds in ground water. *Environmental Science & Technology* 2008, **42**(1)**:** 228–234.

6. Lohmayer R, Kappler A, Lösekann-Behrens T, Planer-Friedrich B. Role of sulfur species as redox partners and electron shuttles for ferrihydrite reduction by Sulfurospirillum deleyianum. *Applied and Environmental Microbiology* 2014**:** AEM. 04220-04213.

7. Couture RM, Rose J, Kumar N, Mitchell K, Wallschlager D, Van Cappellen P. Sorption of arsenite, arsenate, and thioarsenates to iron oxides and iron sulfides: a kinetic and spectroscopic investigation. *Environmental Science & Technology* 2013, **47**(11)**:** 5652-5659.

8. Saalfield SL, Bostick BC. Changes in iron, sulfur, and arsenic speciation associated with bacterial sulfate reduction in ferrihydrite-rich systems. *Environmental Science & Technology* 2009, **43**(23)**:** 8787-8793.

9. Jia Y, Bao P, Zhu Y-G. Arsenic bioavailability to rice plant in paddy soil: influence of microbial sulfate reduction. *Journal of Soils and Sediments* 2015, **15**(9)**:** 1960-1967.

10. De'Ath G. Multivariate regression trees: a new technique for modeling species-environment relationships. *Ecology* 2002, **83**(4)**:** 1105-1117.

11. Planer-Friedrich B, Franke D, Merkel B, Wallschläger D. Acute toxicity of thioarsenates to Vibrio fischeri. *Environmental Toxicology and Chemistry* 2008, **27**(10)**:** 2027-2035.

12. Suess E, Mehlhorn J, Planer-Friedrich B. Anoxic, ethanolic, and cool – An improved method for thioarsenate preservation in iron-rich waters. *Applied Geochemistry* 2015, **62:** 224-233.